NATIONAL PHYSICAL LABORATORY

Anisotropy of Emission from Radionuclide Neutron Sources

by

A G Bardell, M Burke, J B Hunt, H Tagziria, and D J Thomas

Centre for Ionising Radiation Metrology

Abstract.
Radionuclide neutron sources provide a convenient means of producing standard neutron calibration fields for a wide variety of neutron measuring devices. The properties of a source which are required to be known for the characterisation of the field at a point are: the total neutron emission rate, the neutron energy spectrum, and the variation of the intensity of the emission with angle. It is assumed that the variation of the spectrum with angle is negligible for most applications. The total emission rate from radionuclide neutron sources can be measured absolutely at the National Physical Laboratory, NPL, by the manganese sulphate bath technique, or comparatively via a moderating detector. The neutron energy spectra for a variety of commonly used sources are available in the open literature. This report describes the method used at NPL for the measurement of the anisotropic emission from radionuclide neutron sources. The measured neutron angular distributions relative to the cylindrical axes of a variety of source types and encapsulations are given. Also presented are the distributions as calculated using the Monte Carlo transport code MCNP, which in general show good agreement with the measured distributions.

ISSN 1369-6793

National Physical Laboratory
Teddington, Middlesex, UK, TW11 0LW

Approved on behalf of Managing Director NPL, by Dr Julian Hunt
Director, Centre for Ionising Radiation Metrology.

CONTENTS

Page

1. INTRODUCTION

The provision of standard neutron fields with accurately known characteristics, which can be used for the calibration of neutron measuring devices, presents a number of problems. The two characteristics of the field which in general need to be known are the neutron fluence, and the spectral distribution of the neutrons. For radiation protection applications, the relevant dosimetric quantities are conventionally derived directly from the fluence using conversion coefficients appropriate to the particular spectrum.

Monoenergetic neutron fields can be produced by charged particle accelerators using appropriate target materials and accelerated ion beams. This approach, although versatile and necessary for characterising the energy response of devices, requires a suitable particle accelerator, with all the associated hardware, and is thus complex and expensive. Standard fields can also be produced using nuclear reactors, but these again require a considerable investment in hardware.

An alternative and simpler method of producing standard neutron fields, particularly for the routine checking and calibration of devices, is the use of radionuclide neutron sources. Outlined below are a number of advantages of using such sources.

- They are convenient, and in general simpler to use than an accelerator or reactor.
- They have a steady and predictable output which varies only slowly with time. Corrections for this variation can be made using the known half-lives of the radionuclides concerned.
- The total neutron emission from the source can be accurately known, to better than 1%[1] it has been measured using the manganese sulphate bath method. Provided this datum is available, and also that the anisotropy of the source emission is known, no additional standardising measurements are necessary at the point of use.
- The sources are reasonably small and portable, allowing calibrations to be made at different locations, for example, for installed monitoring equipment.
- A variety of neutron energy spectra are available, most of which are reasonably well known, and which are routinely used for dosemeter calibration for protection purposes.
- By using an appropriate shape of source capsule, the neutron emission can be almost isotropic, although measurement of the angular variation still needs to be performed to obtain the highest accuracy.

The properties of these radionuclide neutron sources which have to be known if they are to be used for the provision of standard neutron fields are: the total neutron emission rate, the angular variation of emission with respect to the axis of the source (these two are needed to derive the fluence at any distance and angle), and the energy spectrum of the neutrons emitted by the source. After a brief discussion of emission rate measurements, and the types of spectra available, this report concentrates on the determination of the angular variation of the emission, conventionally known as the anisotropy of the neutron emission.

---

1 All uncertainties quoted in this report are estimates of standard (1σ) uncertainties representing a confidence level of approximately 67% unless otherwise stated.

2. TOTAL NEUTRON EMISSION

Radionuclide neutron source emission rates have been measured at the NPL by the manganese sulphate bath method for more than thirty years as part of the Measurement Services of the Centre for Ionising Radiation Metrology[1,2]. The technique involves locating the source at the centre of a large, 1 m or 0.5 m diameter, spherical vessel containing an aqueous solution of manganese sulphate in which the emitted neutrons are slowed down to thermal energies and a known fraction are subsequently captured by the $^{55}Mn(n,\gamma)^{56}Mn$ reaction. The amount of radioactive manganese produced is proportional to the source emission rate, and the induced activity is measured by pumping the solution past two scintillation detectors, the γ-counting efficiencies of which have been determined using absolutely calibrated ^{56}Mn solution. The accuracy of the technique has been validated by international intercomparison[3].

All radionuclide sources used at NPL for the provision of standard neutron fields have been calibrated by the manganese sulphate method. The service is available to customers on a fee paying basis and is used by industry, research laboratories, universities and hospitals. Additionally, a number of different source types are available for short term leasing both within the UK and overseas.

Radionuclide sources calibrated at NPL are in use throughout the UK and in many countries overseas. These sources, together with knowledge of their neutron energy spectra, form the basis of the calibration of other secondary standard instruments such as the precision long counter, and are extensively used for the calibration of all types of neutron detectors, especially area survey instruments and personal dosemeters.

3. NEUTRON ENERGY SPECTRA

Radionuclide neutron sources offer a range of broad energy spectra. In general these spectra are difficult and time consuming to measure because the available spectrometers are limited by energy resolution, dynamic range, low detection efficiency, or any combination of these. The exception to this is the ^{252}Cf spectrum which has been accurately characterised by time-of-flight methods. (Practical californium sources contain approximately 80% ^{252}Cf and 20% ^{250}Cf. The implications of this for the spectrum are small, but there is a greater effect on the effective half-life which increases as the source ages.) Most users employ published neutron energy spectra[4-8], in particular those specified by the International Organisation for Standardization (ISO)[9].

The most commonly used sources for instrument calibration are ^{252}Cf (spontaneous fission) and $^{241}Am\text{-}Be(\alpha,n)$, having mean neutron energies, $\underline{E}$, of 2.1 MeV and 4.2 MeV respectively. Sources with alternative mean neutron energies are also available including: $^{241}Am\text{-}B(\alpha,n)$ ($\bar{E}$ of 0 .8 MeV), $^{241}Am\text{-}F(\alpha,n)$ ($\bar{E}$ of 1.5 MeV), and $^{241}Am\text{-}Li(\alpha,n)$ ($\bar{E}$ of 0.5 MeV).

If a neutron energy spectrum is required which extends from the MeV region down to near thermal energies, such as might be encountered in a practical radiation protection situation, then it is possible to use a moderated ^{252}Cf source spectrum[9]. This is achieved in the laboratory by placing a ^{252}Cf source at the centre of a 30 cm diameter sphere of heavy water (D_2O), which is covered with 1 mm thick cadmium metal to remove the thermal neutron component.

Other neutron energies, generally in fairly narrow distributions, are available by using photoneutron (γ,n) sources such as ^{24}Na-Be ($\bar{E}$ of 0.95 MeV), ^{226}Ra-Be ($\bar{E}$ of 0.35 MeV), or ^{124}Sb-Be ($\bar{E}$ of 0.022 MeV). However, the advantages of these narrow energy range sources is greatly outweighed by the very high intensity gamma radiation field which they produce, several orders of magnitude greater than the neutron field, which makes their use very difficult anywhere other than inside a heavily shielded room. Their short half-lives, with the exception of ^{226}Ra, also means that reactivation in a nuclear reactor is required before use.

4. MEASUREMENT OF ANISOTROPIC EMISSION

Commercially available radionuclide neutron sources are generally cylindrical in shape and, due to the need for robust and safe encapsulation, are inhomogeneous in construction. The net result is that they do not emit neutrons with equal intensity in all directions, and cannot therefore be considered as truly isotropic sources. The total neutron emission, as measured by the manganese sulphate bath, cannot thus, on its own, be used to calculate accurately the neutron fluence at a point distant from the source. Information must also be available on the anisotropy of emission.

4.1 Measurement method

For anisotropy measurements at NPL the source is placed at the centre of a low-scatter area with its cylindrical axis in the horizontal plane. Neutron emission rates are measured, using a long counter, over the angular range 0° to 180° relative to the cylindrical axis of the source, in steps of 10°. The physical arrangement is shown in Figure 1. Over the years measurements of source anisotropy have been made with two long-counters. One is an NPL adaptation of the McTaggart design, the second a De Pangher precision long-counter. Both counters have been found to give consistent results. The NPL long-counter has the advantage of a counting efficiency which is a factor of three higher than the De Pangher.

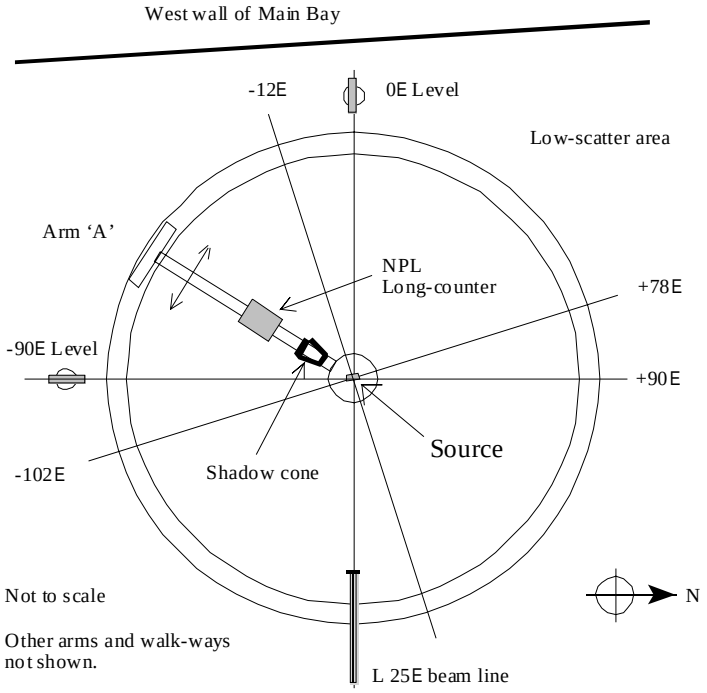

Figure 1. Experimental arrangement for measuring anisotropy of emission from radionuclide neutron sources in the NPL low-scatter area.

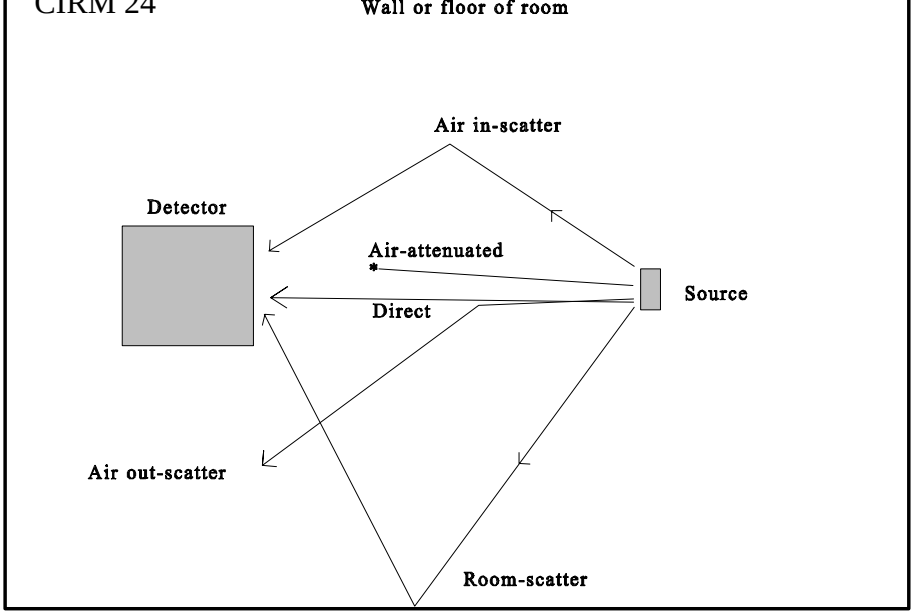

Figure 2. Room scattering processes.

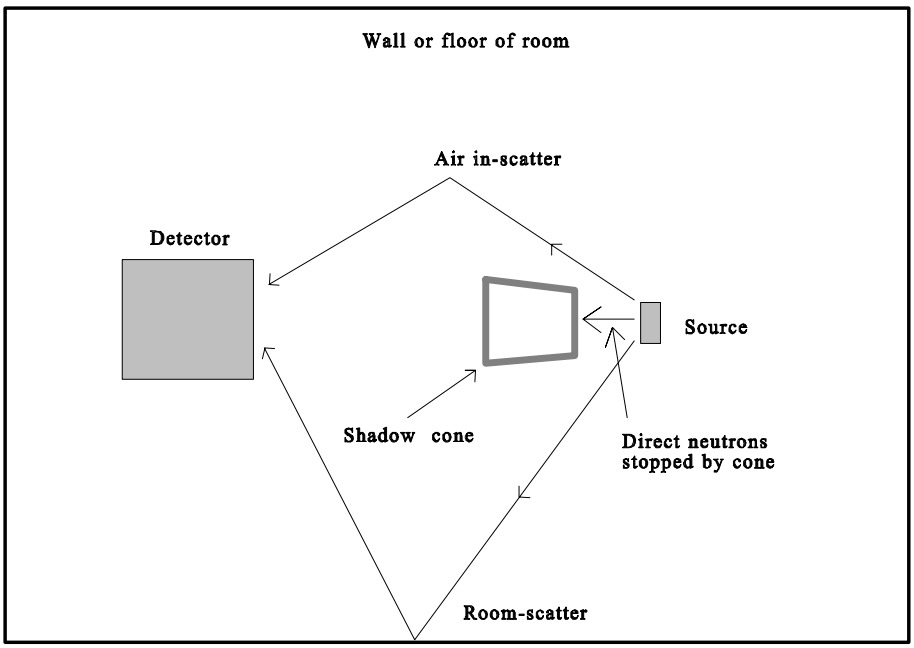

Figure 3. Shadow cone measurements.

All laboratory measurements made with neutron sources, radionuclide or accelerator produced, suffer from the interfering effects of neutrons scattered from the surrounding surfaces, support materials, and the air. The processes are illustrated in Figure 2. To correct for the scattered component measurements are taken at each angle both with, and without, a shadow cone present between the source and the long counter, see Figure 3. By subtracting the measurement with the shadow cone from the total measurement, the air in-scatter and room scatter is estimated. Corrections are also applied for dead-time and out-scatter of neutrons by air between the source and the long counter[10].

The distance between the source and the long counter is conventionally set to about 2 m. A number of considerations influence the choice of this distance. Bringing the counter closer to the source would decrease the size of the scatter correction. Also, it would increase the count rate, hence improving the statistical accuracy obtained in a fixed counting period. Due to the finite size of the long counter, however, it measures the emission averaged over a range of angles. Even for a 2 m separation distance the angle subtended by the sensitive area of the long counters used at NPL is about 5.7°. Bringing the counter closer to the source would further increase this angular range. A distance of 2 m thus provides a reasonable compromise, although smaller distances sometimes have to be used for low-output sources.

Ideally, anisotropy measurements are made with the detector-to-source distance kept constant, and the detector transport system at NPL achieves this with variations of only about 1 mm while the angle is varied over the range 0° to 180°. Measurements with a dummy source in position allow these small variations to be determined and corrections applied if necessary.

4.2 Calculation of the anisotropy factors

For anisotropically emitting neutron sources, the neutron fluence $\varphi(r,\theta,\alpha)$, at a distance r, and at angle $\Omega(\theta,\alpha)$, is related to the total source emission, B, by the double integral:

$$B = \int_{\alpha=0}^{2\pi} \int_{\theta=0}^{\pi} \phi(r,\theta,\alpha) r^2 \sin\theta \, d\theta \, d\alpha \qquad (1)$$

The spherical coordinate system in which the angles are defined is shown schematically in Figure 4.

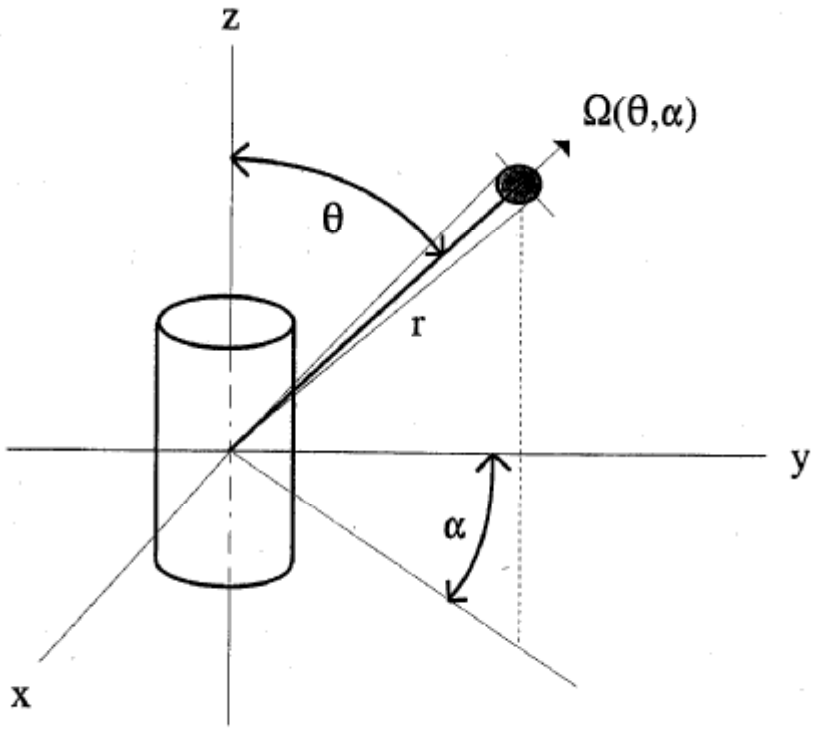

Figure 4. System of spherical co-ordinates for neutron emission from a source: taken from Reference 9.

If the neutron emission is independent of the azimuthal angle α, i.e. the source has rotational symmetry about its cylindrical axis, then the following simpler relationship will hold:

$$B = 2\pi r^2 \int_{\theta=0}^{\pi} \phi(r,\theta) \sin\theta \, d\theta \qquad (2)$$

This simpler relationship applies in all practical situations and will be assumed throughout the rest of this derivation. (See also Section 11).

The anisotropy factor, $F_I(\theta)$, may be defined as the ratio of the neutron fluence at a point on a line through the centre of the source, and making an angle θ with respect to the axis of the cylindrical source, to the fluence averaged over all points located at the same distance from the centre of the source. Then, the neutron fluence rate in free space at a point (r,θ) may be expressed by:

$$\phi(r,\theta) = \frac{B F_1(\theta)}{4\pi r^2} \qquad (3)$$

In practice the source to detector distance r is large enough (usually of the order of 2 m) for the effects of finite source and detector sizes to be unimportant.

Substituting equation (2) into equation (3) leads to:

$$F_I(\theta) = \frac{2\,\phi(r,\theta)}{\int_{\theta=0}^{\pi} \phi(r,\theta) \sin\theta \, d\theta} \qquad (4)$$

Thus, if the neutron fluence rate $\phi(r,\theta)$ as a function of the neutron emission angle θ is known at a fixed separation distance r, then the anisotropy correction factor, $F_I(\theta)$, at any emission angle θ can be calculated. The neutron fluence anisotropy factor may be determined experimentally with a neutron sensitive device whose response is energy-independent, or nearly so. The fluence response of the NPL long counters have been shown to be sufficiently energy-independent for them to be used, not only for intercomparing the emission rates of neutron sources with the same neutron energy spectra, but also of sources with slightly different spectra. Since the expected changes in the neutron energy spectrum, due to scattering within the source, as a function of the emission angle θ are small, any small departures from a strictly energy-independent response should introduce negligible effects upon the measured anisotropy factors.

In this case, the detector count-rate, $C(r,\theta)$, at a neutron emission angle θ and distance r may be expressed by:

$$C(r,\theta) = \bar{\varepsilon}\, \phi(r,\theta) \qquad (5)$$

where $\bar{\varepsilon}$ is the average response of the detector to neutrons from a particular source in terms of counts per unit neutron fluence (i.e. cm^2). Substituting equation (5) into equation (4) leads to:

$$F_I(\theta) = \frac{2\,C(r,\theta)}{\int_{\theta=0}^{\pi} C(r,\theta)\sin\theta\,\delta\theta} \qquad (6)$$

Since both functions in the integrand are continuous and do not change their sign within the integration limits, the integral can be replaced by a summation and the anisotropy factors, $F_I(\theta_m)$, for each measurement angle θ_m, can be calculated using the expression:

$$F_I(\theta_m) = \frac{2\,C(\theta_m)}{\sum_{i=1}^{19} C(\theta_i)\,[\cos((\theta_{i-1}+\theta_i)/2) - \cos((\theta_{i+1}+\theta_i)/2]} \qquad (7)$$

where $C(\theta_i)$ is the count rate at angle θ_i at some fixed constant distance r, corrected for scatter and dead time effects. The angles θ_1 and θ_{19} are taken as 0° and 180° respectively for the above formula, and θ_i extends from 0° to 180° in steps of 10° corresponding to i increasing from 1 to 19. The term:

$$[\cos((\theta_{i-1}+\theta_i)/2) - \cos((\theta_{i+1}+\theta_i)/2)] \qquad (8)$$

is the solid angle factor at angle θ_i. Angles θ_0 and θ_{20} are taken to be 0° and 180° respectively, so that the first and last terms in the summation cover the angular intervals 0° to 5° and 175° to 180° respectively. The other terms cover angular intervals of 10°, i.e. 5° to 15°, 15° to 25°, etc. The measurements are performed at the mid point of the angular intervals, except for the first and last intervals where the measurements are at 0° and 180° respectively rather than 2.5° and 177.5°. The consequences of this for the overall results are negligibly small since the total solid angle factor is very small for the first and last intervals.

Greater importance is usually attached to determining the anisotropy factor at 90°, $F_I(90)$, because this is the most commonly used direction for detector calibration, and the angle at which the change of emission with angle is usually a minimum. Measurements are therefore performed for longer at this angle in order to reduce the statistical uncertainty.

5. DESCRIPTION OF THE SOURCES MEASURED

5.1 Source types

The main objective of this work was to determine the anisotropy of emission for as wide a variety of source types as was possible in the available time. Advantage was also taken of the availability of some duplicate sources with the same type of encapsulation to permit comparisons between the anisotropies of nominally identical sources.

The sources measured fall into three main categories:

a) ^{252}Cf spontaneous fission sources in different encapsulations where the ^{252}Cf was either deposited in solution and evaporated to dryness, or was in the form of a wire alloy.

b) ^{241}Am-Be(α,n) sources in four different encapsulations where the ^{241}Am as an oxide powder is mixed with the powdered target material (Be) and compressed into pellets which are a close fit in the inner capsule.

c) other ^{241}Am sources with neutron producing target materials of boron, fluorine, lithium with similar construction to that described for b).

Categories a) and b) form the most commonly used and readily available types of radionuclide source used as secondary standards. Category c) consists of rather more exotic and less common source types which are sometimes used because of their lower mean neutron energies. The main characteristics of all the sources measured are given in Table 1.

Table 1. The main characteristics of the sources measured.

Source type	Nominal activity or mass	Encapsulation style	Diameter (mm)	Height (mm)	Nominal neutron emission rate (s^{-1})	Manufacturer	Table no.	Figure no.
^{252}Cf (sp.fis.)	10 μg	X1 (A)	7.8	10.0	2.5 H 10^{7}	AI [1]	2	7
^{252}Cf (sp.fis.)	10 μg	X1 (B)	7.8	10.0	2.5 H 10^{7}	AI	3	8
^{252}Cf (sp.fis.)	0.1 μg	X224	9.4	32.5 [2]	2.0 H 10^{5}	AI	4	9
^{252}Cf (sp.fis.)	17 μg	SR-Cf-100	9.4	32.5 [2]	4.0 H 10^{7}	S R [3]	5	10
^{241}Am-Be (α,n)	100 mCi	X2	17.4	19.4	2.5 H 10^{5}	AI	6	11
^{241}Am-Be (α,n)	1 Ci	X3 (A)	22.4	31.0	2.5 H 10^{6}	AI	7	12
^{241}Am-Be (α,n)	1 Ci	X3 (B)	22.4	31.0	2.5 H 10^{6}	AI	8	13
^{241}Am-Be (α,n)	3 Ci	X4	22.4	48.5	7.5 H 10^{6}	AI	9	14
^{241}Am-Be (α,n)	5 Ci	X14 (A)	30.0	60.0	1.3 H 10^{7}	AI	10	15
^{241}Am-Be (α,n)	10 Ci	X14 (B)	30.0	60.0	2.5 H 10^{7}	AI	11	16
^{241}Am-Be (α,n)	10 Ci	X14 (C)	30.0	60.0	2.5 H 10^{7}	AI	12	17
^{241}Am-Be (α,n)	15 Ci	X14 (D)	30.0	60.0	3.8 H 10^{7}	AI	13	18
^{241}Am-B (α,n)	1 Ci	X3	22.4	31.0	4.4 H 10^{5}	AI	14	19
^{241}Am-F (α,n)	1 Ci	X3	22.4	31.0	1.4 H 10^{5}	AI	15	20
^{241}Am-Li (α,n)	5 Ci	X14	30.0	60.0	2.1 H 10^{5}	AI	16	21
^{239}Pu-Li (α,n)	17 Ci	2729-C	38.0	52.3	1.1 H 10^{6}	Monsanto [4]	17	22

1. Originally *The Radiochemical Centre*, subsequently *Amersham International plc*, later *Nycomed Amersham plc*, now *AEA Technology QSA* a business within AEA Technology plc.
2. Including an additional threaded stud 5.0 mm long at one end.
3. Savannah River Laboratory.
4. Monsanto Research Corporation

Note: Mention of particular commercial products does not in any way imply recommendation or endorsement by the National Physical Laboratory.

Radionuclide sources based on (α,n) reactions are conventionally manufactured and sold with activities which are nominally integral numbers of curies, milli-curies, or micro-curies. Such sources have long been referred to by quoting the activity of the α-particle emitting radionuclide in curies (1 Ci is equivalent to 37 GBq). Although the curie is not the SI unit of activity, these sources continue to be referred to in terms of the activity in curies since this provides a very convenient label.

5.2 Encapsulation

For radiological safety reasons radionuclide neutron source material is securely encapsulated in order to contain the active elements. Commercially available sources are doubly encapsulated, and are sufficiently robust to pass several stringent tests. The safety assessment and classification of sealed radioactive sources is covered by ISO standard ISO 2919 - 1980. For neutron sources this recommends a minimum classification of '43334'. This five figure code indicates the severity of tests in the areas of: temperature, external pressure, impact, vibration, and puncture. Typically the sources used in this study have classifications of '66545' which exceeds the minimum.

The material used to encapsulate the active components of the source modifies the emitted neutron angular distribution and energy spectrum. The material used should therefore be selected with the aim of minimising the macroscopic capture and scatter cross sections, and be as thin as possible consistent with safe containment. Most commercially available sources are cylindrical in shape with a height to diameter ratio in the range of 1 to 2. Several of them incorporate a means of attachment, usually a threaded recess or stub, and this complicates the shape. The path-lengths of the emitted neutrons within the source and its encapsulation thus vary with position of generation and angle of emission relative to the axis of the source. Both the source material and the encapsulation can cause scattering. The net result is that the source does not emit neutrons equally in all directions and cannot be considered as a point source. Figure 5 provides a schematic illustration of all the source capsules for which measurements are reported here.

In general, the most commonly used ^{252}Cf spontaneous fission sources and the smaller ^{241}Am(α,n) sources, are encapsulated in thin stainless steel, have no added means of attachment, have a height to diameter ratio approaching unity, and are the most isotropic sources available.

6. SOURCE HOLDERS AND EXPERIMENTAL DETAILS

All source anisotropy measurements made at NPL are performed in a large low-scatter laboratory approximately 25 m long, 18 m wide, and 18 m high. Sources are located to one end of this room at a position 6 m above the floor at the centre point of a 12 m diameter pit. The advantage of using a large room is the reduction in the fraction of source neutrons scattered from the room surfaces and subsequently detected in the long-counter being used. The use of a light floor and minimal support structures further reduces the effect.

The long-counter used to make the measurements is mounted on a carriage attached to an arm one end of which can rotate about a fixed point at the centre of the pit. The outer end of the arm runs on a circular horizontal track at a distance of approximately 5 m from the centre pivot. The carriage can be positioned at known distances from the centre of rotation of the arm. Both rotation and distance can be controlled remotely. This arrangement enables a series of measurements to be made at known angles with respect to the cylindrical axis of a source placed above the centre of rotation with its axis in the same horizontal plane as the long counter. There is provision to mount a shadow cone above the inner end of the arm, between the source and the long counter, thus always shadowing the long counter as it is rotated about the source.

The source is held in the horizontal position on a small aluminium "V" holder mounted on a stand above the centre of rotation. The amount of supporting material close to the source is kept to a minimum to reduce the effects on the measurement of scatter from the support. The general arrangement is shown in plan view in Figure 1.

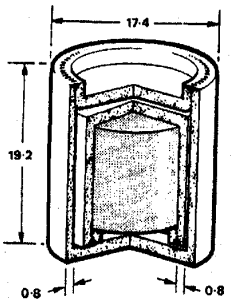

X2

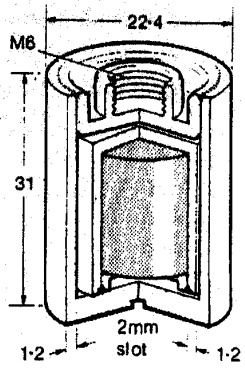

X3

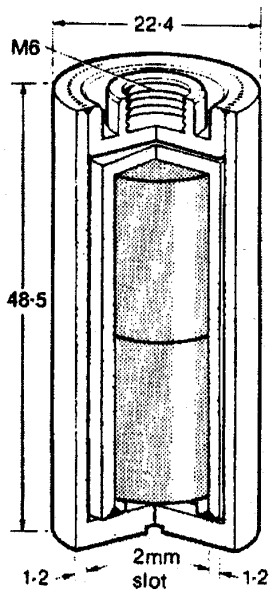

X4

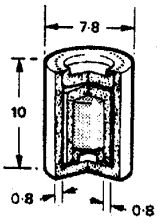

X1

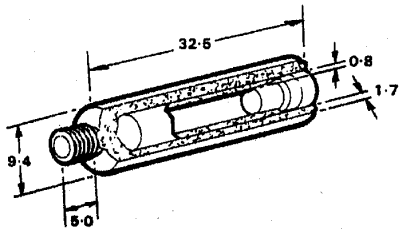

X224 - external dimensions identical for SR-Cf-100

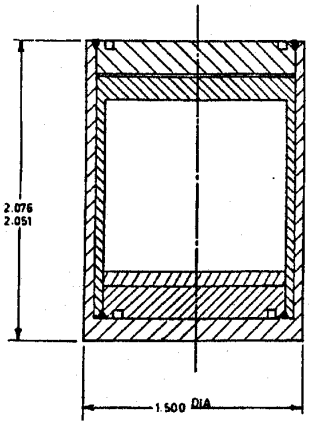

Monsanto 2729-C

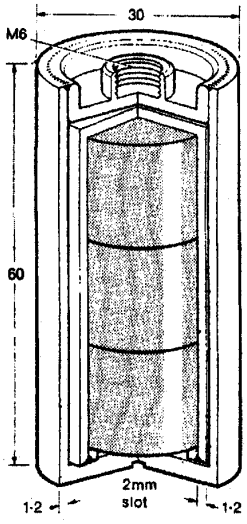

X14

Figure 5. Schematic representation of typical source encapsulations. Dimensions are in mm for the X capsules and inches for the Monsanto capsule. Diagrams not to scale.

To ensure that the shadow cone fully shadows the long counter at all angles, and that the measurement distance remains constant, it is essential that the source is mounted with its active centre, i.e. the centre of the active material within the encapsulation, accurately above the centre of rotation of the arm. Alignment of the source is achieved by the use of a plumb-bob, suspended from a wire which is precisely positioned above a line between the centre of rotation of the arm and the 0° reference angle at the outer end of the track[2], and two surveyors optical 'levels'. The following sequence of operations ensure correct alignment of the source on its support.

a) The plumb-bob is attached to the wire and positioned so that its point is accurately above the centre of rotation of the arms. Alignment of the plumb-bob string is checked using the level at the 0° reference position. This level is permanently mounted at the 0° position at the working height for the detectors. A second level is then positioned outside the track in the 90° direction and the eyepiece centred on the plumb-bob string. The two levels now define the centre position for the source.

b) The plumb-bob is removed and the source holder on its support column is mounted so that it is exactly at the centre of rotation. See Figure 6 (a) and (b) for a diagrammatic indication of the views through the eyepieces of the two levels. A dummy source capsule with the same external dimensions as the source to be measured is placed on the "V" and the height adjusted if necessary, see Figure 6 (c) and (d). The dummy source capsule carries a mark to indicate the active centre, and the capsule is orientated so that the mark is clearly visible through the level at the 0° reference position. The capsule is next positioned so that the active centre mark is aligned with the cross-wires of the 0° level. Because of the way the "V" holder has been set up, the cylindrical axis of the source is then at 90° to the 0° reference direction.

c) An appropriate shadow cone is selected; a simple graphical computer program is available to help with this, and mounted on its support. The distance between the cone and the source is chosen to ensure complete shadowing of the source at the measurement distance. Some guidance on the selection and use of shadow cones is given in NPL Report RS 5[10].

d) The arrangement of arms and walk-ways relative to the 0° reference direction necessitates the 180° measurement scan around the source being made over angles from -102° to +78° on the track, so the source cylindrical axis needs to be aligned along this direction. The level at the -90° position is moved to -102° and the source on its "V" holder rotated until the source axis is aligned at -102°. This becomes the 0° pole direction for the anisotropy measurement, cf. the angles used in the description of the analysis in Section 4.2. Next, the level at 0° is rotated until the cross wires line up with a clearly visible edge on one end of the source, see Figure 6(e). It is necessary to use an edge because the active sources do not carry an active centre mark.

e) The dummy source is removed and the source to be measured is carefully placed on the "V"holder such that it lines up with the cross wires in the 0° level. The source is now set up for the measurement.

2 The angles referred to in this section are those marked on the outer end of the track supporting the moveable arms. The reference angle of 0° corresponds to the direction of the left -25° beam line from the NPL 3.5 MV Van de Graaff accelerator.

View through levels with source on “V” holder in correct position

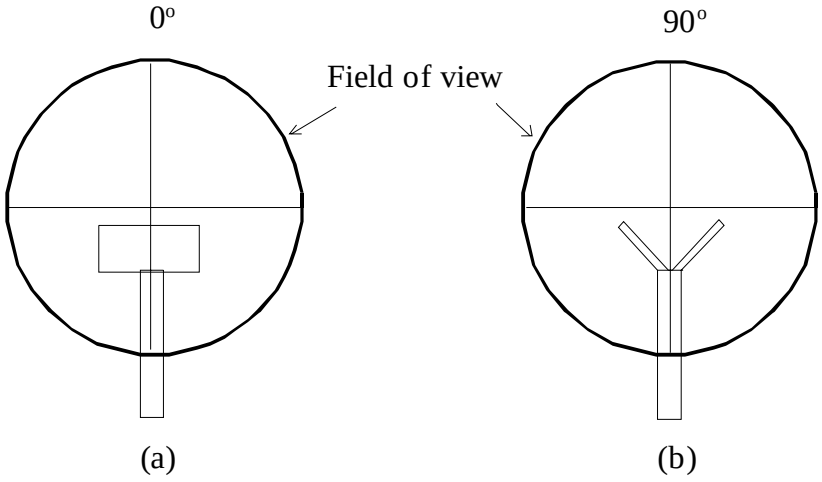

View through levels with source on “V” holder in correct position

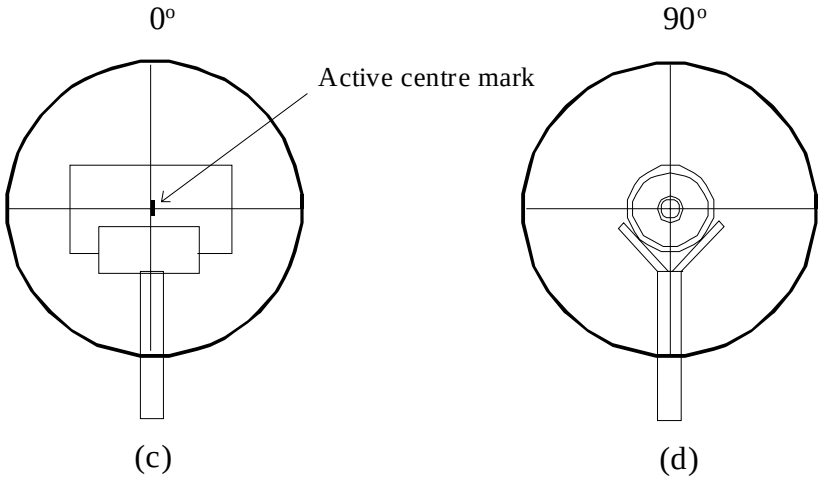

View through 0º level with source rotated to the -102º direction

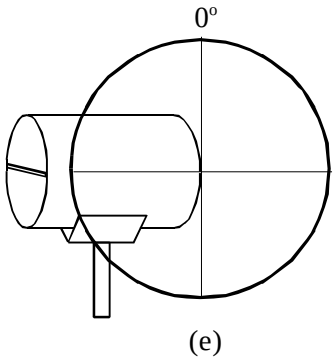

Figure 6. Source positioning and alignment.

7. MEASUREMENTS AND ANALYSIS

Since the process of setting up the shadow cone to ensure proper alignment, i.e. complete shadowing of the long-counter, involves viewing the system from a position close to the source, this is best done with the dummy source in position. It is then convenient to perform the first set of measurements with the cone present, taking care not to disturb the cone after setting up with a dummy source. Measurements are started with the long counter at -102° and proceed in 10° steps through an arc of 180° to +78°.

The cone is then removed from its support, a quick and simple operation, and the direct measurements are made in the reverse direction.

It is desirable to make at least three measurements at each angle so that the uncertainty derived from the spread of results can be compared to that expected from Poisson statistics. Whenever possible measurements are made to an accuracy approaching 0.1% at each angle.

The counting period required is determined from knowledge of the source emission rate and the long-counter efficiency. Time constraints, particularly when measuring a low emission rate source, may limit the duration of the counting period. Since the most commonly used direction when the source is used for irradiations is at 90° relative to the source cylindrical axis it is desirable to make extra measurements in this direction to reduce the uncertainty on $F_I(90°)$.

The resulting total and shadowed counts, with their counting periods, and the source to long counter distances, form the input data for a computer program, ANISOT, which calculates the anisotropy factors for each angle of measurement according to equation (7). Also required as input is an estimate of the air attenuation factor for the source-to-detector distance used. For a particular neutron energy, the air-attenuation factor can be obtained from a knowledge of the total neutron cross sections for nitrogen and oxygen at that energy[11]. For radionuclide sources, which have a broad neutron spectrum, average attenuation correction factors need to be calculated by folding the factor as a function of neutron energy with the source spectrum. Values for ^{252}Cf sources, both bare and heavy-water moderated, and for ^{241}Am-Be and ^{241}Am-B can be found in reference 11. Values for the other sources were calculated using the best available spectral data.

8. RESULTS

Tables 2 to 17 give the values of the anisotropy factors $F_I(\theta_m)$, at intervals of 10° relative to the cylindrical axis, for the sources listed in Table 1. The quoted uncertainty is that due to statistics only, and is estimated at the 67% (1σ) confidence level. Other components, for example, due to distance variations with changing angle, or slight movements of the source, are expected to be negligible compared to the statistics.

The 0° angle corresponds to the end of the source having the closing weld. For the X3, X4, and X14 capsules this corresponds to the end having a recessed screw thread, while for X224/SR-Cf-100 capsules it is the ‘plain’ end. Neutron emission is assumed to be symmetrical about the cylindrical axis of the source, see Section 11.

Graphical representations of the results is provided by Figures 7 to 22, which give linear plots of the same tabulated data. The line drawn through each set of $F_I(\theta_m)$ values is a guide for the eye only, and does not in any way represent a fit to the data.

Table 2. Anisotropy factors for a 10 μg X1 encapsulated ^{252}Cf source measured at 10° intervals. This source was made by depositing the californium from solution, and the activity is believed to be concentrated at the bottom of the inner capsule. (X1 A)

θ_m°	$F_I(\theta_m)$	Uncertainty
0	1.0267	0.0023
10	1.0274	0.0023
20	1.0166	0.0022
30	1.0107	0.0022
40	1.0058	0.0022
50	0.9959	0.0021
60	0.9956	0.0021
70	0.9802	0.0021
80	0.9848	0.0021
90	1.0103	0.0011
100	1.0157	0.0021
110	1.0190	0.0021
120	1.0119	0.0021
130	1.0037	0.0021
140	0.9880	0.0022
150	0.9805	0.0022
160	0.9647	0.0022
170	0.9644	0.0022
180	0.9745	0.0023

Quoted uncertainties represent the statistical components only, and are at the 67% (1σ) confidence level.

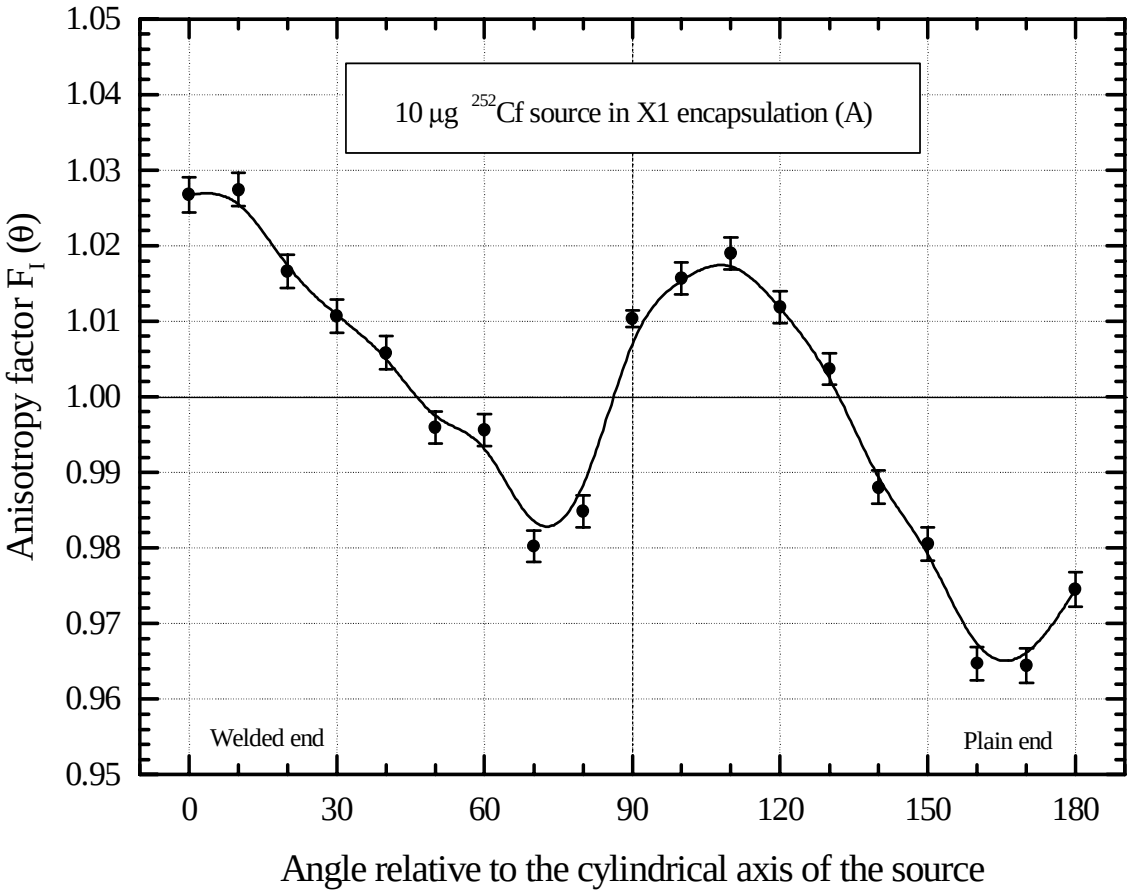

Figure 7. Anisotropy factors for X1 encapsulated ^{252}Cf source (A): data from Table 2.

Note: the source was produced by deposition of the ^{252}Cf from solution, and the activity is believed to be concentrated at the welded end.

Table 3. Anisotropy factors for a 10 μg X1 encapsulated ^{252}Cf source measured at 10° intervals. The ^{252}Cf material is in the form of a wire alloy which has been centralised within the capsule using an inner bobbin. (X1 B)

θ_m°	$F_I(\theta_m)$	Uncertainty
0	1.0055	0.0030
10	1.0035	0.0030
20	0.9968	0.0029
30	0.9704	0.0028
40	0.9667	0.0028
50	0.9890	0.0028
60	1.0063	0.0028
70	1.0164	0.0028
80	1.0146	0.0027
90	1.0176	0.0022
100	1.0159	0.0027
110	1.0139	0.0028
120	1.0071	0.0028
130	0.9911	0.0028
140	0.9688	0.0028
150	0.9723	0.0028
160	0.9912	0.0029
170	1.0056	0.0027
180	1.0018	0.0030

Quoted uncertainties represent the statistical components only, and are at the 67% (1σ) confidence level.

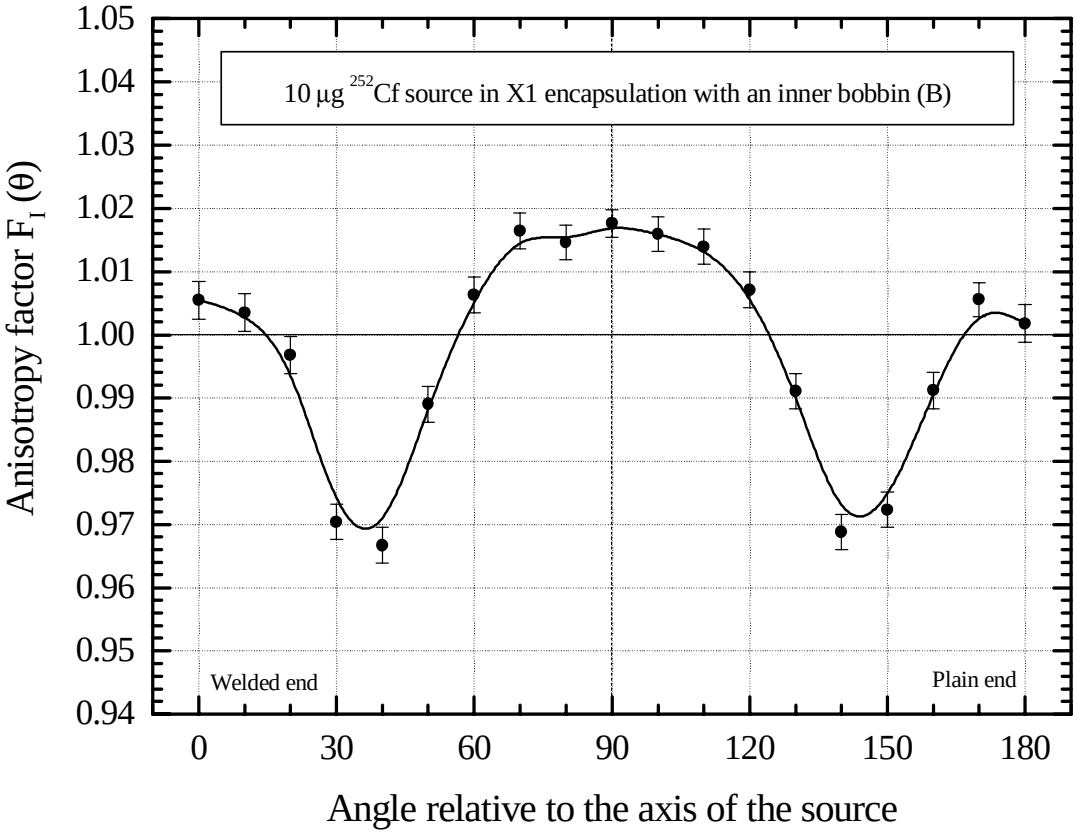

Figure 8. Anisotropy factors for X1 encapsulated ^{252}Cf source (B): data from Table 3.

Note: the source includes an inner bobbin which locates the wire alloy containing the ^{252}Cf at the centre of the source capsule.

Table 4. Anisotropy factors for a 0.1 μg X224 encapsulated ^{252}Cf source measured at 10° intervals.

θ_m°	$F_I(\theta_m)$	Uncertainty
0	0.8877	0.0031
10	0.9272	0.0046
20	0.9936	0.0049
30	1.0035	0.0078
40	0.9941	0.0077
50	0.9953	0.0075
60	1.0079	0.0047
70	1.0097	0.0075
80	1.0176	0.0070
90	1.0198	0.0034
100	1.0125	0.0074
110	1.0264	0.0075
120	1.0294	0.0076
130	1.0102	0.0076
140	0.9910	0.0035
150	0.9656	0.0077
160	0.9076	0.0076
170	0.7617	0.0073
180	0.8005	0.0040

Quoted uncertainties represent the statistical components only, and are at the 67% (1σ) confidence level.

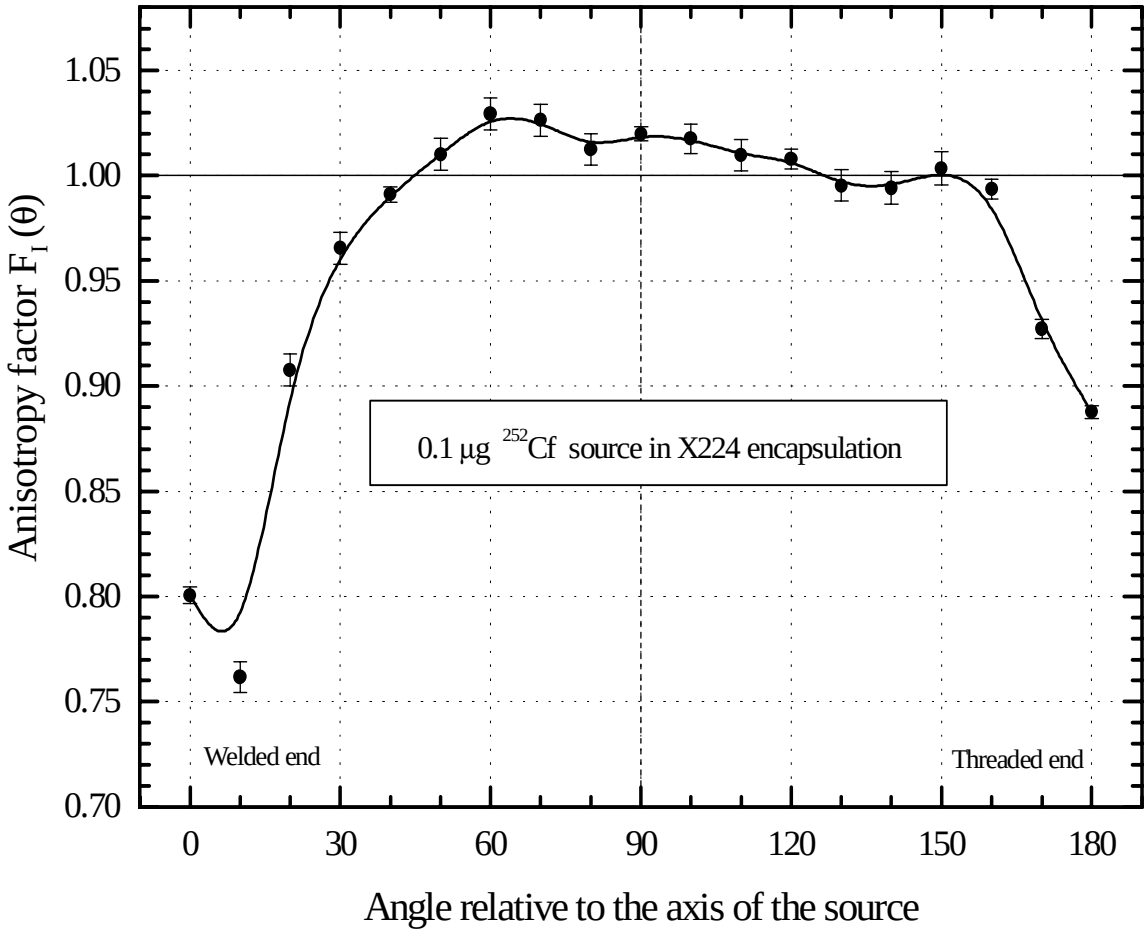

Figure 9. Anisotropy factors for an X224 encapsulated ^{252}Cf source: data from Table 4.

Table 5. Anisotropy factors for a 17 μg SR-Cf-100 encapsulated ^{252}Cf source measured at 10° intervals.

θ_m°	$F_I(\theta_m)$	Uncertainty
0	0.7948	0.0021
10	0.8285	0.0143
20	0.8872	0.0012
30	0.9537	0.0038
40	0.9921	0.0029
50	1.0122	0.0012
60	1.0213	0.0016
70	1.0271	0.0016
80	1.0306	0.0053
90	1.0348	0.0026
100	1.0366	0.0012
110	1.0333	0.0015
120	1.0264	0.0017
130	1.0116	0.0017
140	0.9875	0.0014
150	0.9454	0.0071
160	0.8689	0.0063
170	0.8156	0.0182
180	0.8215	0.0016

Quoted uncertainties represent the statistical components only, and are at the 67% (1σ) confidence level.

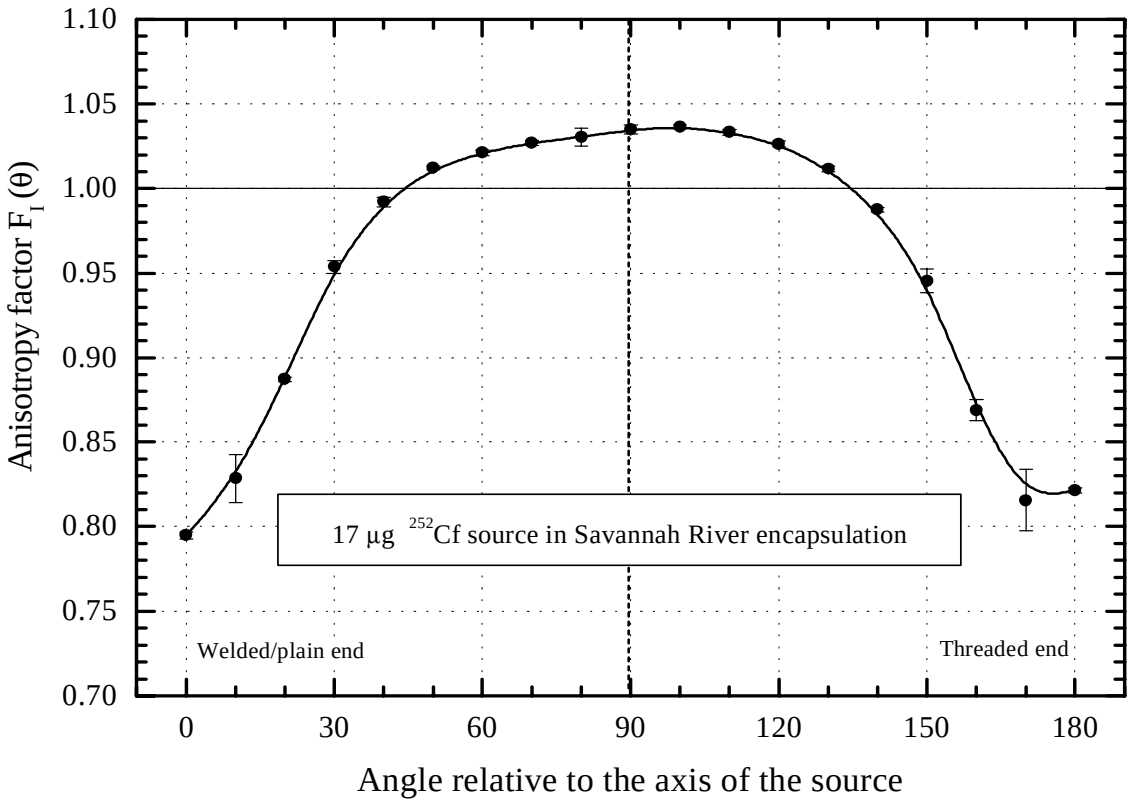

Figure 10. Anisotropy factors for a Savannah River encapsulated 17 µg ^{252}Cf source: data from Table 5.

Table 6. Anisotropy factors for an X2 encapsulated 100m Ci ^{241}Am-Be source measured at 10° intervals.

θ_m°	$F_I(\theta_m)$	Uncertainty
0	1.0243	0.0097
10	1.0182	0.0094
20	1.0235	0.0093
30	1.0124	0.0091
40	1.0091	0.0100
50	0.9891	0.0098
60	0.9735	0.0096
70	1.0069	0.0087
80	1.0146	0.0087
90	1.0112	0.0037
100	1.0111	0.0087
110	1.0210	0.0087
120	0.9946	0.0088
130	0.9887	0.0098
140	0.9652	0.0098
150	0.9639	0.0089
160	0.9984	0.0092
170	0.9902	0.0093
180	1.0369	0.0096

Quoted uncertainties represent the statistical components only, and are at the 67% (1σ) confidence level.

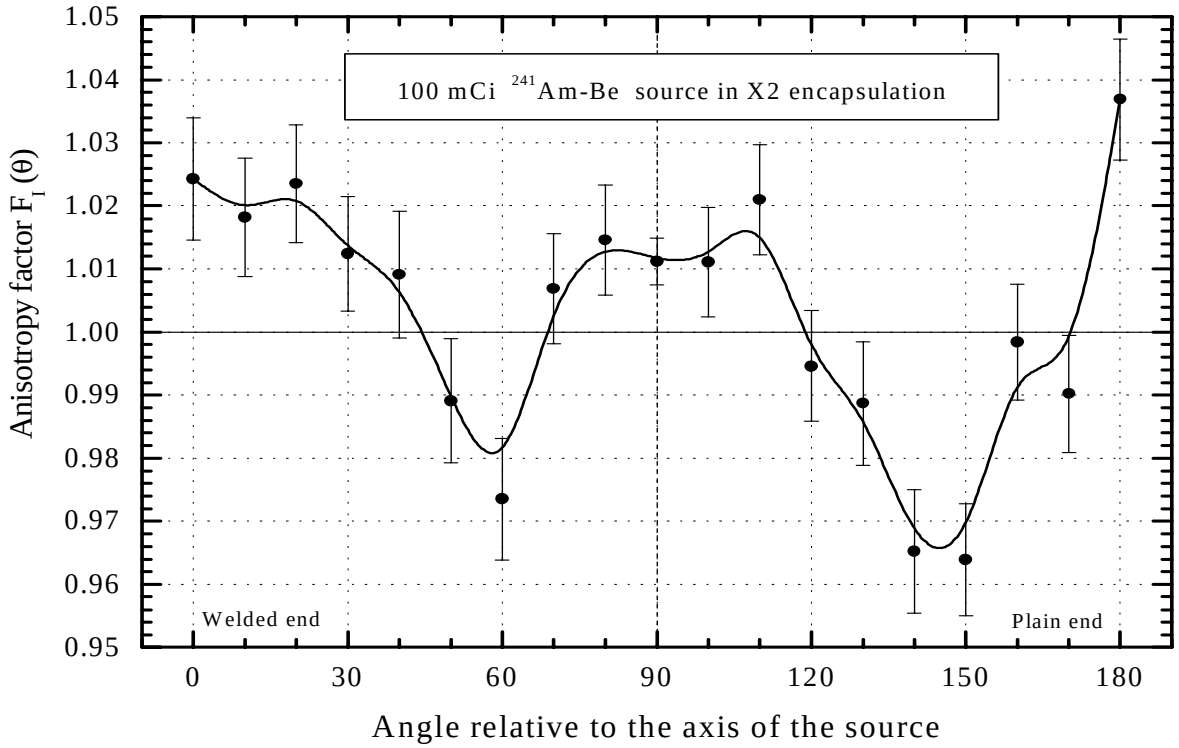

Figure 11. Anisotropy factors for an X2 encapsulated 100 mCi ^{241}Am Be source: data from Table 6.

Note: the emission rate was low, being approximately 2.5 x 10^5 s^{-1}, resulting in long measurement times with poor statistics.

Table 7. Anisotropy factors for an X3 encapsulated 1 Ci ^{241}Am-Be source measured at 10° intervals. (X3 A)

θ_m°	$F_I(\theta_m)$	Uncertainty
0	0.9949	0.0057
10	0.9804	0.0041
20	0.9640	0.0055
30	0.9700	0.0055
40	0.9885	0.0054
50	0.9857	0.0054
60	1.0100	0 .0054
70	1.0172	0.0054
80	1.0253	0.0054
90	1.0276	0.0028
100	1.0231	0.0047
110	1.0177	0.0050
120	1.0077	0.0052
130	0.9810	0.0054
140	0.9730	0.0054
150	0.9622	0.0054
160	0.9490	0.0055
170	0.9691	0.0041
180	0.9657	0.0057

Quoted uncertainties represent the statistical components only, and are at the 67% (1σ) confidence level.

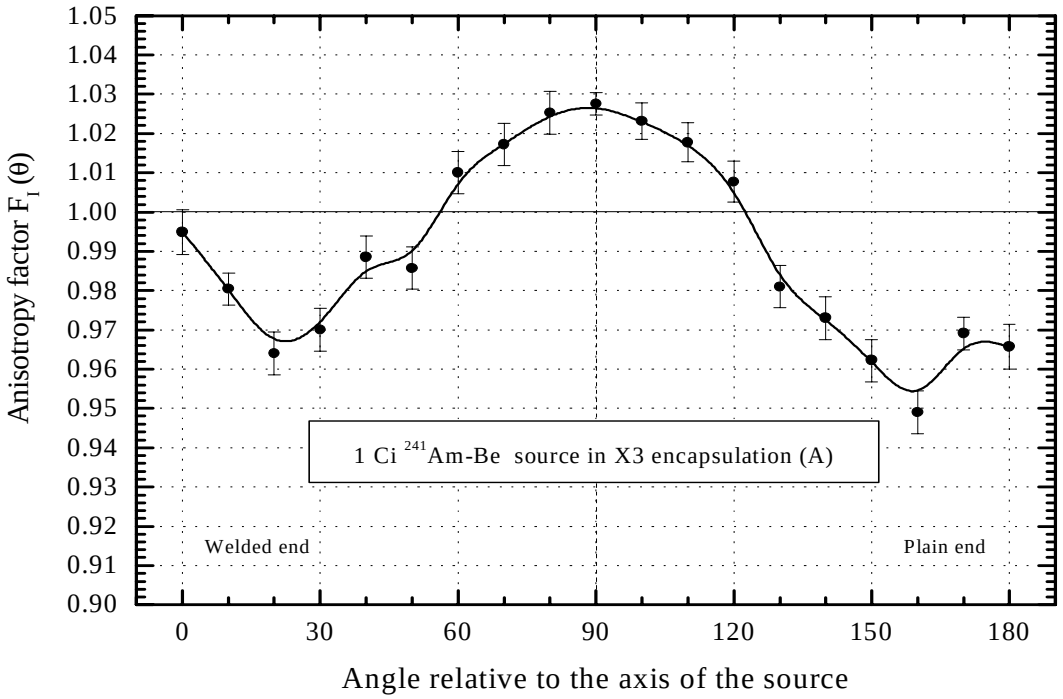

Figure 12. Anisotropy factors for an X3 encapsulated 1 Ci ^{241}Am-Be source (A): data from Table 7.

Table 8. Anisotropy factors for an X3 encapsulated 1 Ci ^{241}Am-Be source measured at 10° intervals. (X3 B)

θ_m°	$F_I(\theta_m)$	Uncertainty
0	0.9888	0.0039
10	0.9748	0.0053
20	0.9633	0.0048
30	0.9708	0.0051
40	0.9741	0.0051
50	0.9932	0.0050
60	1.0168	0.0050
70	1.0162	0.0050
80	1.0235	0.0050
90	1.0265	0.0037
100	1.0235	0.0049
110	1.0095	0.0049
120	1.0032	0.0050
130	0.9899	0.0046
140	0.9724	0.0050
150	0.9650	0.0051
160	0.9713	0.0051
170	0.9576	0.0052
180	0.9802	0.0030

Quoted uncertainties represent the statistical components only, and are at the 67% (1σ) confidence level.

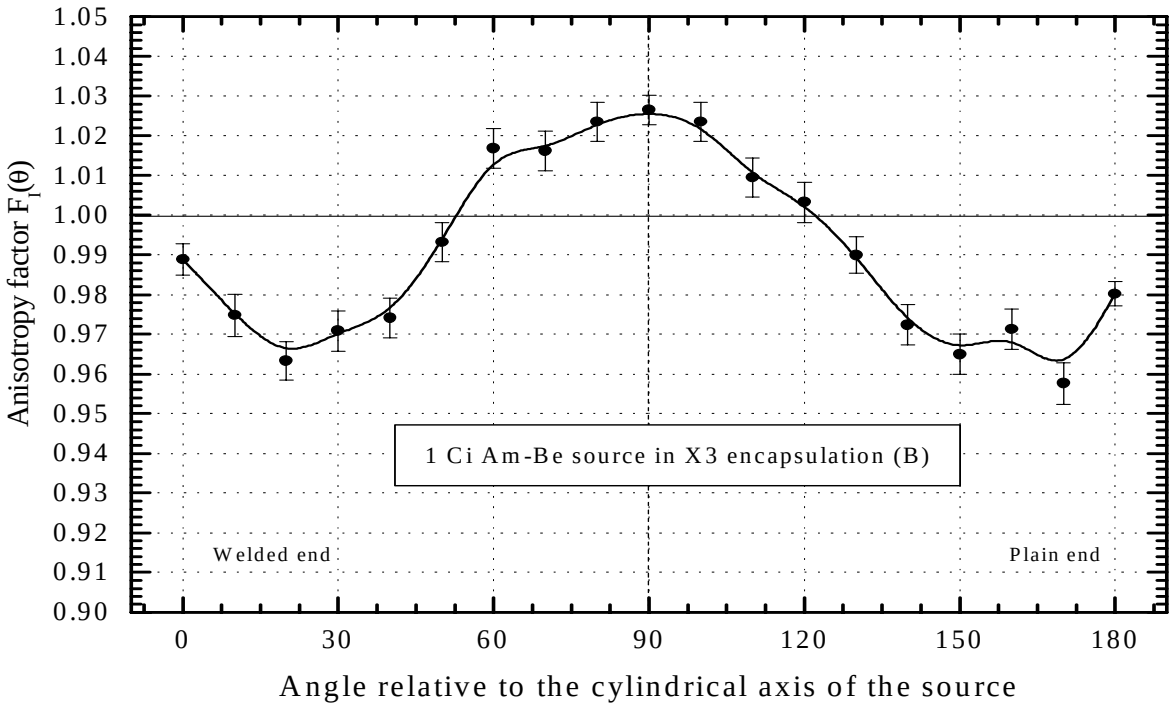

Figure 13. Anisotropy factors for an X3 encapsulated 1 Ci ^{241}Am-Be source (B): data from Table 8.

Table 9. Anisotropy factors for an X4 encapsulated 3 Ci ^{241}Am-Be source measured at 10° intervals.

θ_m°	$F_I(\theta_m)$	Uncertainty
0	0.8746	0.0034
10	0.8700	0.0034
20	0.8976	0.0029
30	0.9369	0.0034
40	0.9703	0.0034
50	1.0008	0.0034
60	1.0193	0.0034
70	1.0343	0.0034
80	1.0393	0.0034
90	1.0436	0.0025
100	1.0435	0.0034
110	1.0289	0.0034
120	1.0220	0.0034
130	1.0029	0.0034
140	0.9748	0.0034
150	0.9363	0.0034
160	0.8934	0.0033
170	0.8578	0.0033
180	0.8619	0.0034

Quoted uncertainties represent the statistical components only, and are at the 67% (1σ) confidence level.

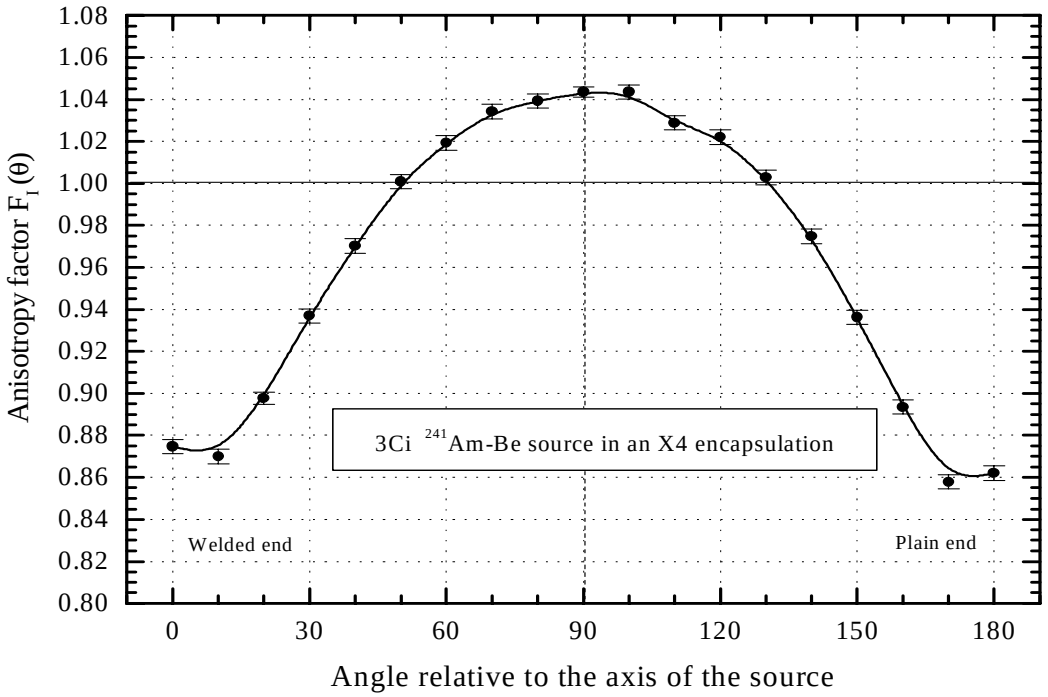

Figure 14. Anisotropy factors for an X4 encapsulated 3 Ci ^{241}Am-Be source: data from Table 9.

Table 10. Anisotropy factors for an X14 encapsulated 5Ci ^{241}Am-Be source measured at 10° intervals. (X14A)

θ_m°	$F_I(\theta_m)$	Uncertainty
0	0.8752	0.0030
10	0.8735	0.0030
20	0.9021	0.0030
30	0.9411	0.0030
40	0.9756	0.0030
50	1.0067	0.0031
60	1.0203	0.0031
70	1.0328	0.0031
80	1.0390	0.0031
90	1.0464	0.0023
100	1.0401	0.0031
110	1.0304	0.0032
120	1.0168	0.0030
130	0.9967	0.0030
140	0.9741	0.0030
150	0.9326	0.0030
160	0.8905	0.0029
170	0.8609	0.0029
180	0.8603	0.0030

Quoted uncertainties represent the statistical components only, and are at the 67% (1σ) confidence level.

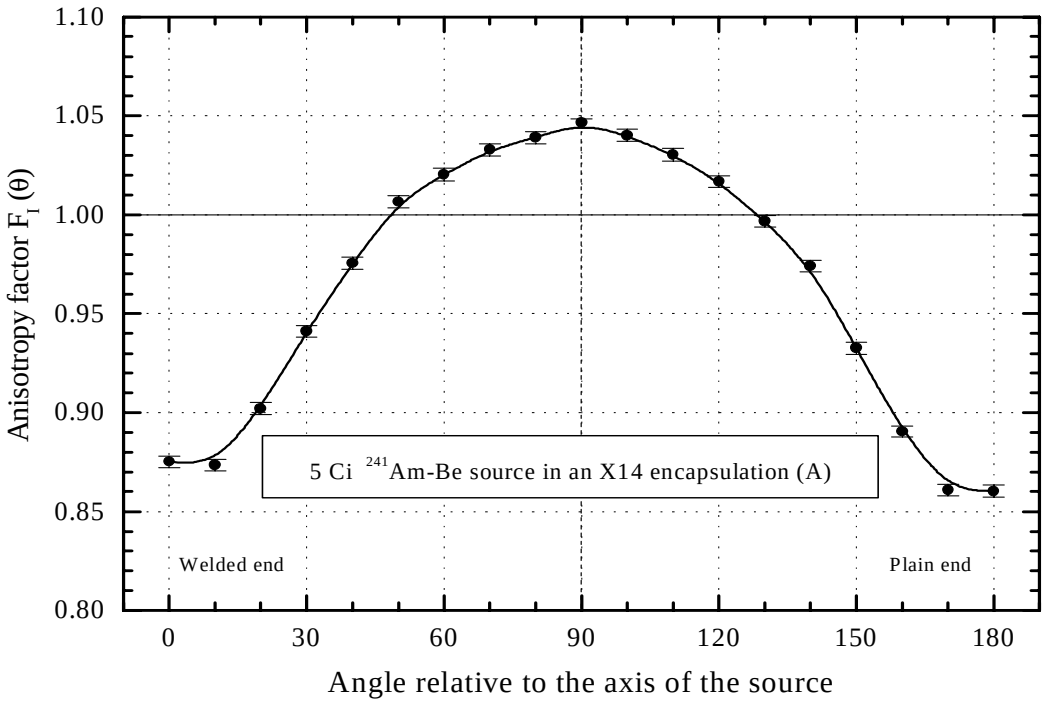

Figure 15. Anisotropy factors for an X14 encapsulated 5 Ci ^{241}Am-Be source (A): data from Table 10.

Table 11. Anisotropy factors for an X14 encapsulated 10Ci ^{241}Am-Be source measured at 10° intervals. (X14B)

θ_m°	$F_I(\theta_m)$	Uncertainty
0	0.8749	0.0024
10	0.8713	0.0023
20	0.8951	0.0023
30	0.9434	0.0023
40	0.9773	0.0023
50	1.0042	0.0023
60	1.0230	0.0023
70	1.0309	0.0023
80	1.0400	0.0023
90	1.0436	0.0013
100	1.0399	0.0023
110	1.0295	0.0023
120	1.0167	0.0023
130	0.9990	0.0023
140	0.9726	0.0023
150	0.9320	0.0023
160	0.8986	0.0023
170	0.8690	0.0023
180	0.8643	0.0023

Quoted uncertainties represent the statistical components only, and are at the 67% (1σ) confidence level.

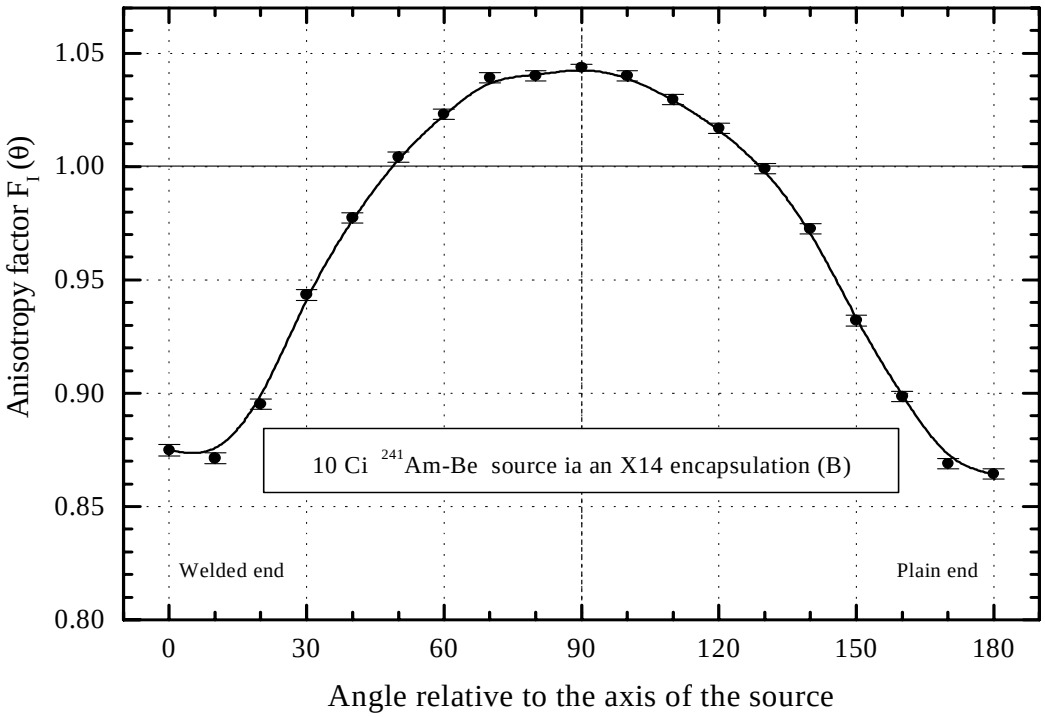

Figure 16. Anisotropy factors for an X14 encapsulated 10 Ci ^{241}Am-Be source (B): data from Table 11.

Table 12. Mean anisotropy factors for an X14 encapsulated 10 Ci ^{241}Am-Be source measured at 10° intervals. (X14C)

θ_m°	$F_I(\theta_m)$	Uncertainty
0	0.9022	0.0010
10	0.8972	0.0031
20	0.9154	0.0026
30	0.9459	0.0013
40	0.9771	0.0024
50	1.0022	0.0013
60	1.0208	0.0024
70	1.0294	0.0013
80	1.0379	0.0013
90	1.0400	0.0009
100	1.0390	0.0013
110	1.0361	0.0013
120	1.0223	0.0013
130	1.0007	0.0028
140	0.9693	0.0020
150	0.9259	0.0013
160	0.8834	0.0026
170	0.8491	0.0024
180	0.8534	0.0033

Quoted uncertainties represent the statistical components only, and are at the 67% (1σ) confidence level.

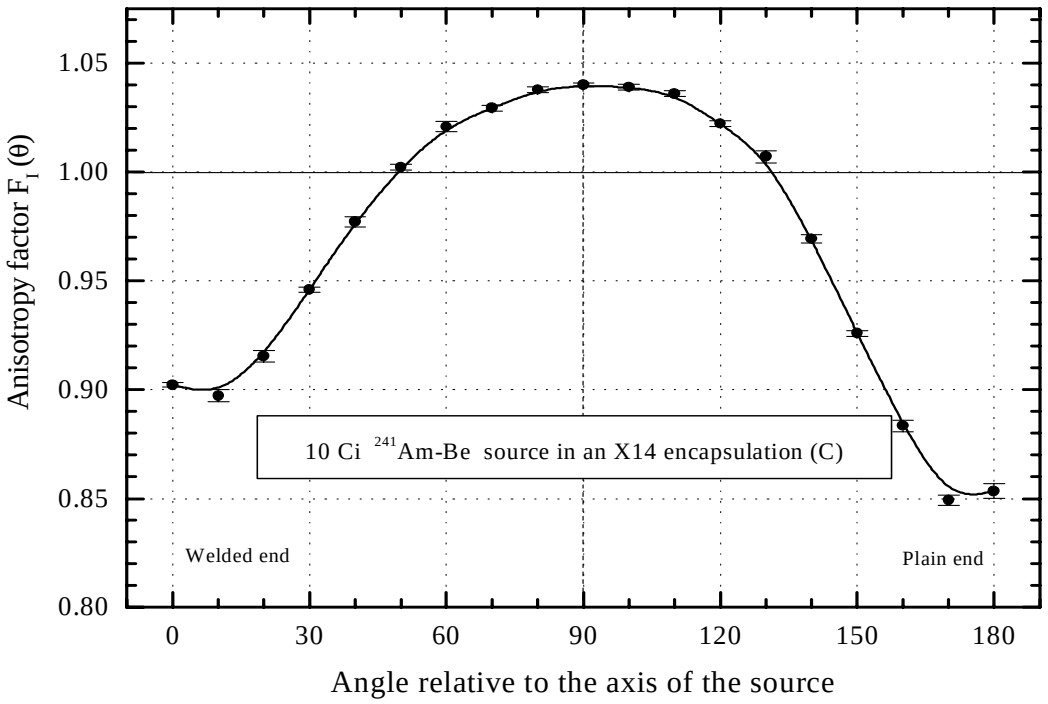

Figure 17. Anisotropy factors for an X14 encapsulated 10 Ci ^{241}Am-Be source (C): data from Table 12.

Table 13. Anisotropy factors for an X14 encapsulated 15 Ci ^{241}Am-Be source measured at 10° intervals. (X14D)

θ_m°	$F_I(\theta_m)$	Uncertainty
0	0.8855	0.0026
10	0.8800	0.0026
20	0.9062	0.0026
30	0.9386	0.0026
40	0.9744	0.0026
50	1.0016	0.0026
60	1.0185	0.0026
70	1.0322	0.0026
80	1.0396	0.0026
90	1.0407	0.0026
100	1.0420	0.0026
110	1.0359	0.0026
120	1.0245	0.0026
130	0.9994	0.0026
140	0.9715	0.0026
150	0.9295	0.0026
160	0.8875	0.0025
170	0.8554	0.0025
180	0.8573	0.0025

Quoted uncertainties represent the statistical components only, and are at the 67% (1σ) confidence level.

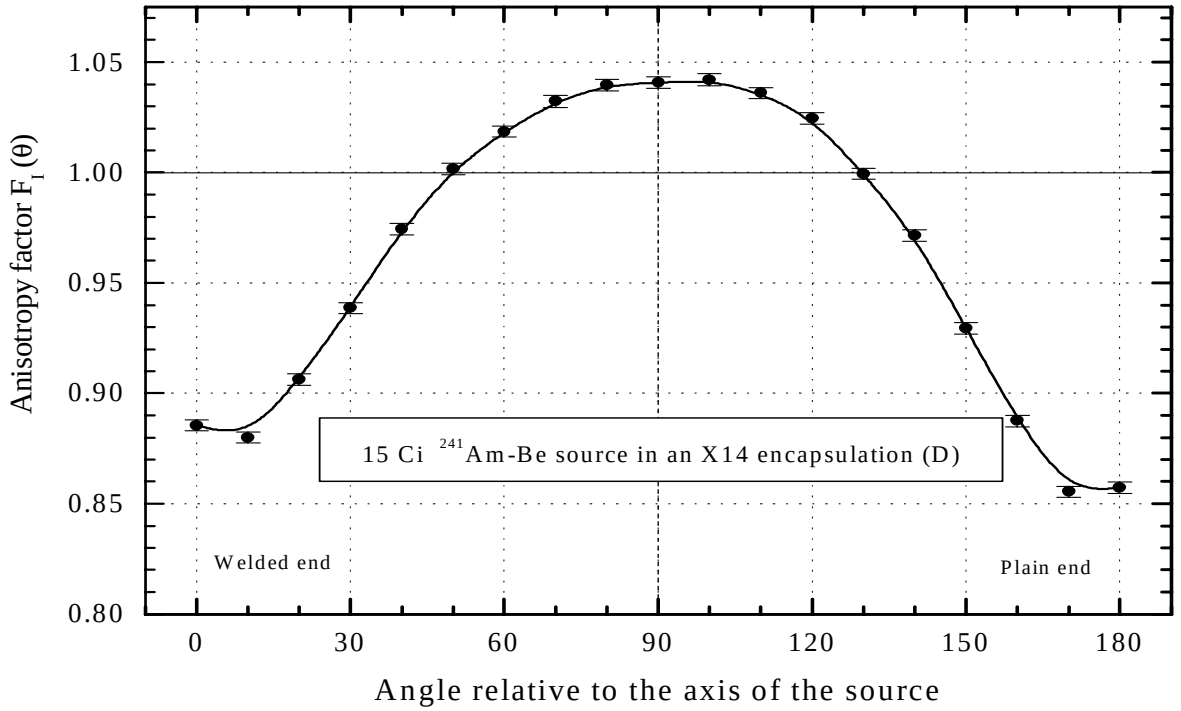

Figure 18. Anisotropy factors for an X14 encapsulated 15 Ci ^{241}Am-Be source (D): data from Table 13.

Table 14. Anisotropy factors for an X3 encapsulated 1 Ci Am-B source measured at 10° intervals.

θ_m°	$F_I(\theta_m)$	Uncertainty
0	0.9839	0.0993
10	0.9688	0.0066
20	0.9844	0.0090
30	0.9671	0.0088
40	0.9849	0.0088
50	0.9758	0.0087
60	1.0114	0.0087
70	1.0178	0.0087
80	1.0232	0.0087
90	1.0345	0.0054
100	1.0111	0.0086
110	1.0126	0.0086
120	1.0117	0.0087
130	0.9992	0.0087
140	0.9753	0.0087
150	0.9579	0.0088
160	0.9540	0.0089
170	0.9604	0.0066
180	0.9583	0.0091

Quoted uncertainties represent the statistical components only, and are at the 67% (1σ) confidence level.

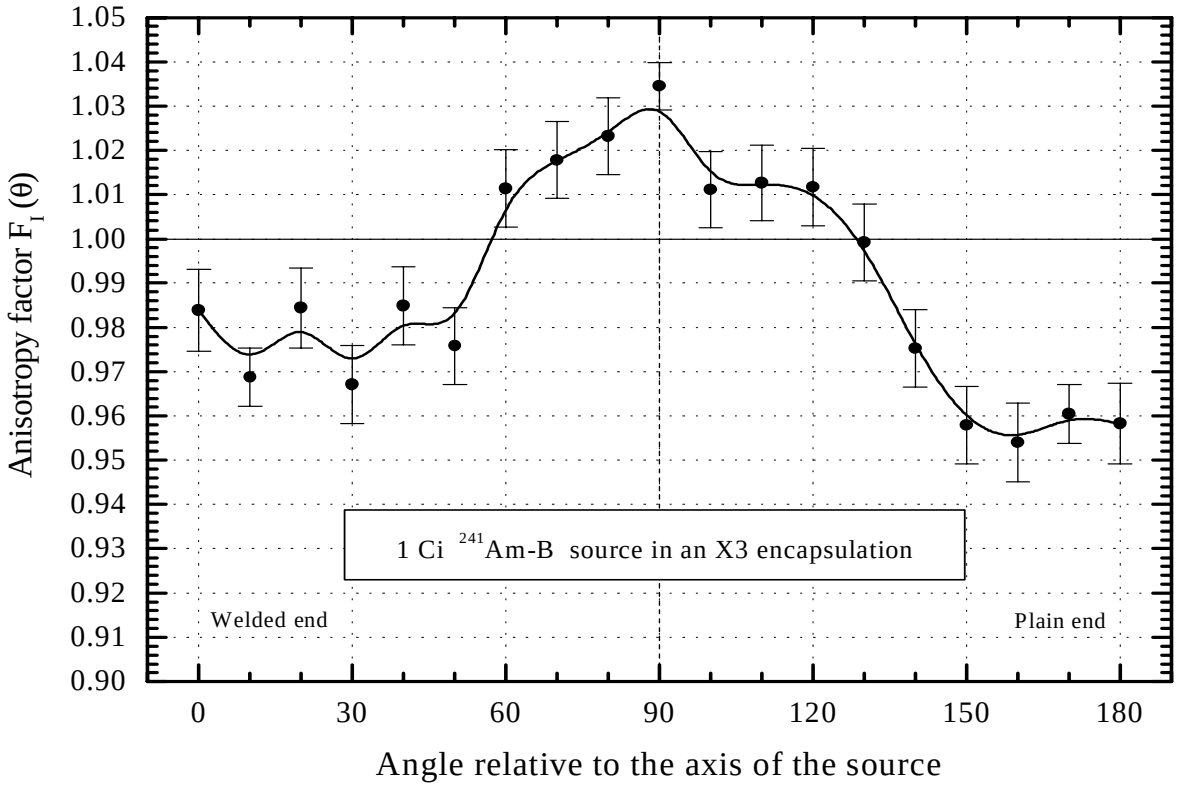

Figure 19. Anisotropy factors for an X3 encapsulated ^{241}Am-B source: data from Table 14.

Table 15. Anisotropy factors for an X3 encapsulated 1 Ci Am-F source measured at 10° intervals.

θ_m°	$F_I(\theta_m)$	Uncertainty
0	0.9838	0.0087
10	0.9714	0.0085
20	0.9491	0.0084
30	0.9666	0.0083
40	0.9910	0.0081
50	0.9810	0.0082
60	1.0181	0.0078
70	1.0278	0.0081
80	1.0205	0.0081
90	1.0224	0.0050
100	1.0326	0.0071
110	1.0193	0.0048
120	1.0047	0.0046
130	0.9836	0.0049
140	0.9632	0.0074
150	0.9524	0.0048
160	0.9628	0.0069
170	0.9701	0.0084
180	0.9532	0.0054

Quoted uncertainties represent the statistical components only, and are at the 67% (1σ) confidence level.

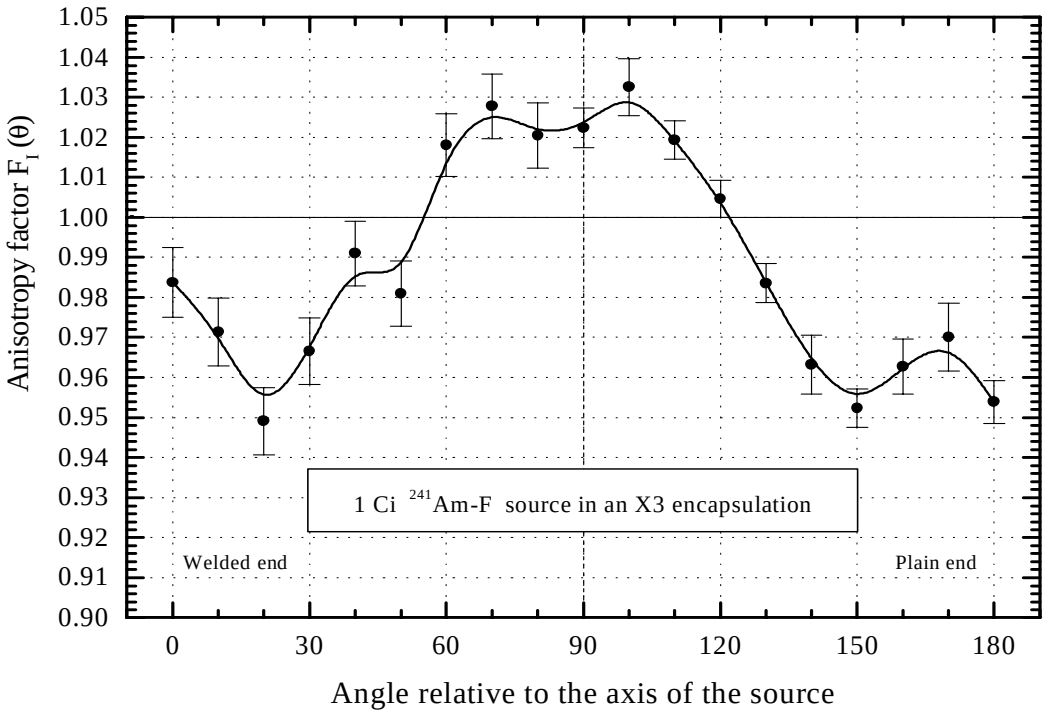

Figure 20. Anisotropy factors for an X3 encapsulated ^{241}Am-F source: data from Table 15.

Table 16. Anisotropy factors for an X14 encapsulated 5 Ci Am-li source measured at 10° intervals.

θ_m°	$F_I(\theta_m)$	Uncertainty
0	0.6899	0.0049
10	0.7080	0.0071
20	0.7737	0.0072
30	0.8438	0.0074
40	0.9220	0.0075
50	0.9749	0.0076
60	1.0382	0.0077
70	1.0692	0.0077
80	1.0915	0.0077
90	1.0760	0.0057
100	1.0712	0.0069
110	1.0641	0.0069
120	1.0477	0.0069
130	1.0124	0.0069
140	0.9671	0.0069
150	0.9000	0.0068
160	0.8483	0.0067
170	0.7981	0.0067
180	0.7633	0.0051

Quoted uncertainties represent the statistical components only, and are at the 67% (1σ) confidence level.

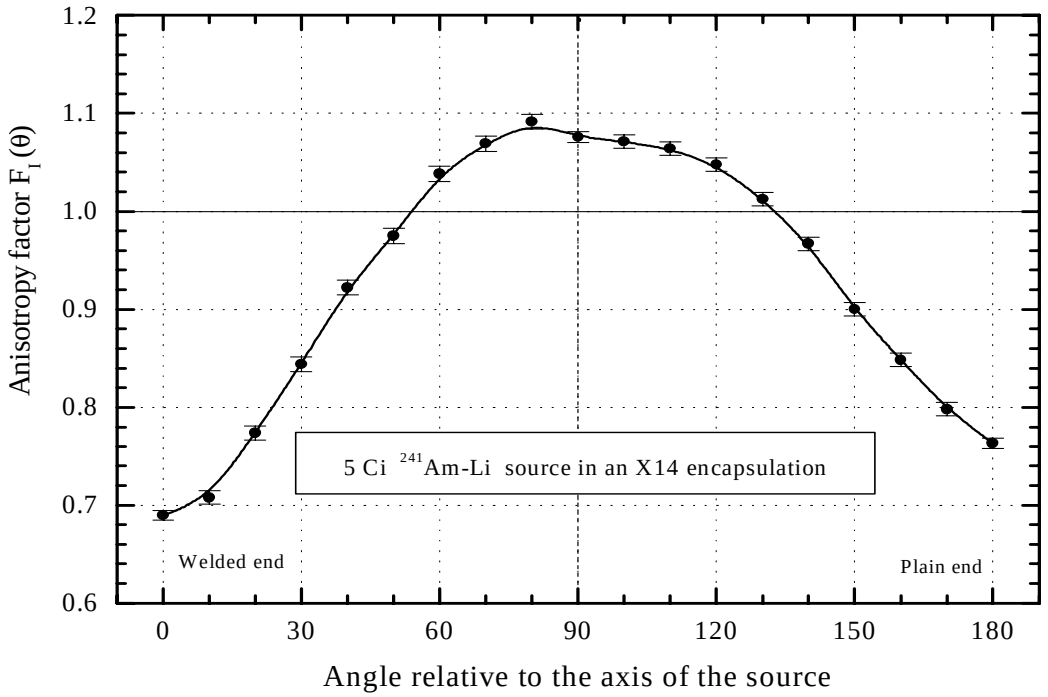

Figure 21. Anisotropy factors for an X14 encapsulated 5 Ci ^{241}Am-Li source: data from Table 16.

Table 17. Anisotropy factors for a Monsanto 2729-C encapsulated 17 Ci ^{238}Pu-Li source measured at 10° intervals.

θ_m°	$F_I(\theta_m)$	Uncertainty
0	0.8532	0.0069
10	0.8781	0.0070
20	0.8924	0.0070
30	0.9365	0.0070
40	0.9500	0.0070
50	0.9882	0.0070
60	1.0293	0.0070
70	1.0556	0.0071
80	1.0771	0.0071
90	1.0777	0.0040
100	1.0690	0.0071
110	1.0504	0.0071
120	1.0110	0.0070
130	0.9697	0.0069
140	0.9238	0.0069
150	0.8821	0.0069
160	0.8411	0.0068
170	0.8128	0.0068
180	0.8138	0.0050

Quoted uncertainties represent the statistical components only, and are at the 67% (1σ) confidence level.

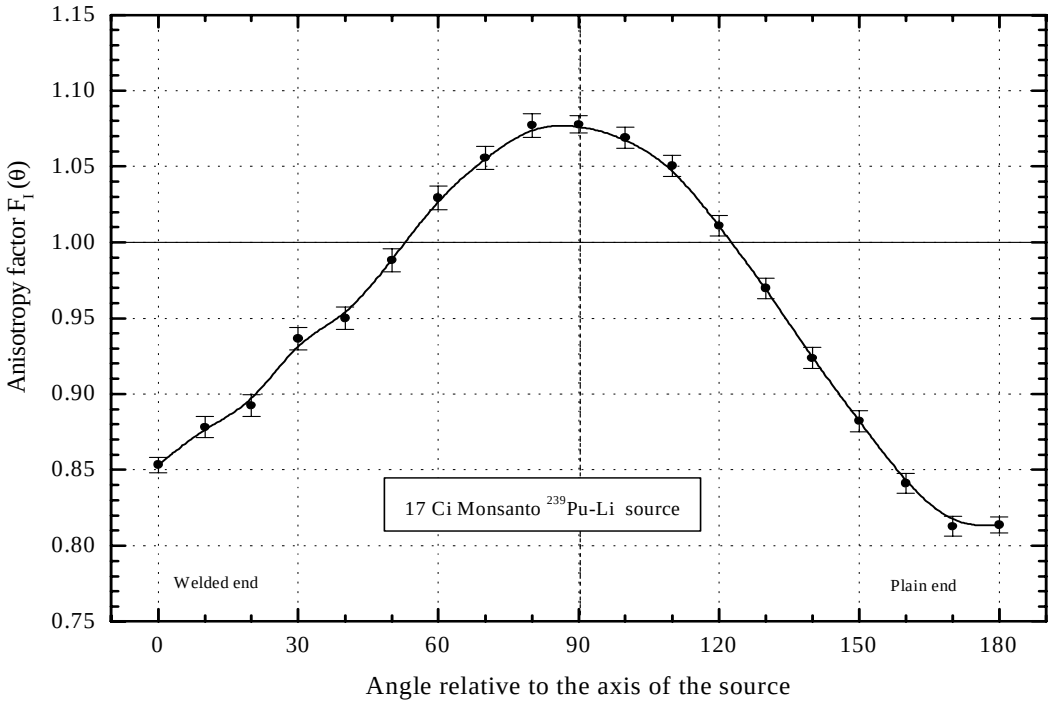

Figure 22. Anisotropy factors for a Monsanto 2729-C encapsulated 17 Ci ^{239}Pu-Li source: data from Table 17.

Very few measurements of radionuclide source anisotropy factors have been reported in the open literature. For the ^{252}Cf sources measured here, there are some calculational results available, but for (α,n) sources based on ^{241}Am, both calculated and measured data are very sparse. For this reason several of the ^{241}Am-Be source encapsulations have been modelled using Monte Carlo techniques and the anisotropy calculated. A discussion of the measured data and comparison with calculation, where available, is delayed until after the section on the Monte Carlo modelling.

9. MCNP MODELLING

The anisotropy factors for X2, X3, and X14 doubly-encapsulated ^{241}Am-Be sources have been calculated using MCNP-4B[12], the latest version of a general purpose Monte Carlo transport code which was written at the Los Alamos National Laboratory in 1943, and has been continuously developed ever since. It is a continuous energy, generalised geometry, time dependent, coupled or de-coupled neutron/photon/electron Monte Carlo code. It is used for radiation transport calculations, and for criticality and reactor physics analyses. The reader is directed to the MCNP-4B manual for a more complete and comprehensive description of the code, how to use it, its physics, cross-section data, and general features.

9.1 The models

The models of the source capsules were constructed from engineering drawings kindly supplied by the manufacturer, and the calculations were performed using the latest ENDF/B-VI cross-section libraries obtained from the NEA data bank for the various materials used to manufacture the source capsules. The neutron spectra used in the calculations were those recommended in ISO Standard 8529[9]. For the X2 and X3 capsules, which contain a single pellet, the neutron source was sampled as isotropic and uniformly distributed in all of the cylindrical inner capsule cell. The X14 capsule is of essentially the same construction as the X3 except that it is larger in size and the active source material consists of three pellets, which can in principle vary in density, packed into the inner capsule, see Figure 5.

9.2 The tallies

MCNP may tally any quantity of the form:

$$C \int \phi(E)\, f(E)\, dE$$

where C is an arbitrary normalisation scaler, $\varphi(E)$ is an energy dependent fluence, and f(E) is either a sum or product of quantities in the cross-section libraries, or it can also be a response function provided by the user.

MCNP calculations of the anisotropy of emission from the sources were performed in two different and independent ways.

In the first method, a segmented surface tally was used. In the language of MCNP input data this involves combining the F2 and FS2 cards. The source was positioned at the centre of a 2 m radius spherical surface which was segmented by 18 parallel planes which divided the sphere surface into a number of smaller surfaces which match those used in the analysis of the measurements. The total fluence through the surface of the sphere was also obtained with the FS2 card approach.

The second method used the 'next event' estimator tally, the so-called 'detector' tally, to calculate the fluence rate at 19 specific angles which matched the angles used in the experimental

measurements with the long counter. In view of the symmetry with respect to the cylindrical axis of the source, the 'ring' detector tally was used instead of the 'point' detector to optimise sampling at all angles other than 0° and 180°. This approach uses the F5 and FY5 cards.

For both methods, all ten MCNP statistical checks were satisfied. The calculations were performed on a personal computer, the surface tally calculations taking about 150 min for 20 million histories on a 166 MHz Pentium machine. The ring/point detector approach took roughly ten times as long for the same number of histories, but resulted in smaller statistical uncertainties. The sources were assumed to be in vacuum for both methods, although some surface tally calculations were also performed with the source in air, and these resulted in almost identical anisotropy factors. This shows that, as expected, the effect of the air on the anisotropy is negligible over distances of a few meters.

The results of method one were used for comparison with measurements, since these provide what is essentially an integration over an angular range, in a similar way to the measurements with a long counter. Calculations using both methods were, however, performed for the three capsules with excellent agreement at all angles with the possible exception of angles near 0° for the X3 and X14 capsules. The probable explanation for this is that the presence of the threaded recess, see Figure 5, results in the fluence at 0° being different to that integrated between 0° and 10°. A comparison of the results of the two methods for the X3 capsule is illustrated in Figure 23. A summary of all the calculated results is given in Table 18. The uncertainties shown are those from the statistics of the Monte Carlo process only.

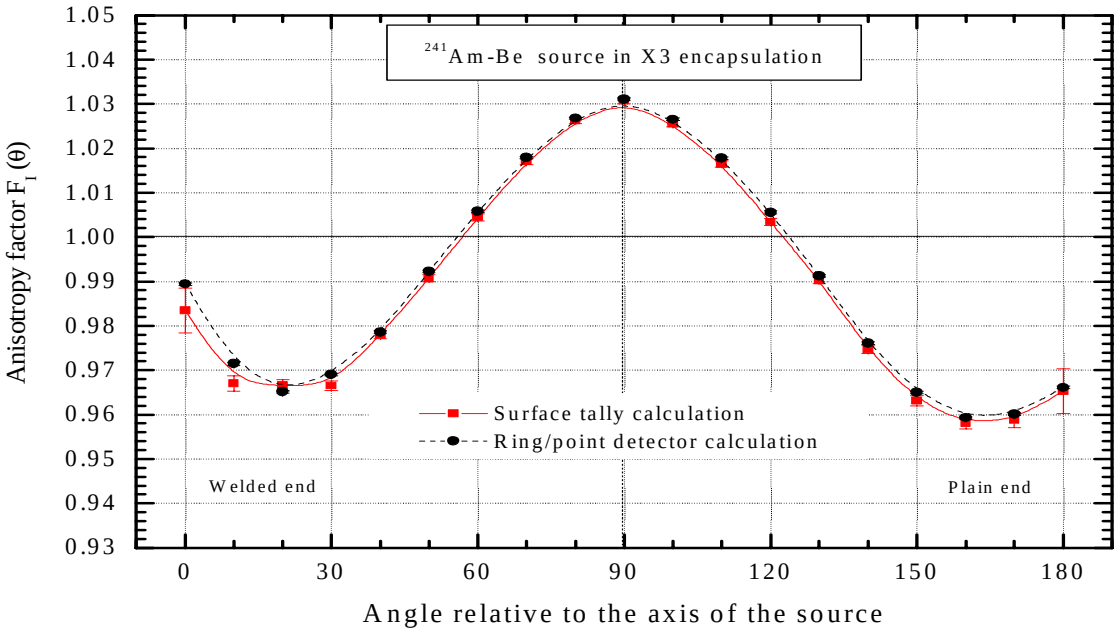

Figure 23. Comparison of surface tally and ring/point detector calculations of the anisotropy for an X3 encapsulated ^{241}Am-Be source.

Table 18. Anisotropy factors calculated using MCNP for X2, X3 and X14 encapsulated ^{241}Am-Be sources.

Angle θ°	X2		X3		X14	
	Surface tally	Detector tally	Surface tally	Detector tally	Surface tally	Detector tally
0	1.0066±0.0051	1.0092±0.0002	0.9854±0.0100	0.9894±0.0003	0.8747±0.0047	0.8756±0.0002
10	0.9982±0.0018	1.0024±0.0003	0.9616±0.0035	0.9714±0.0003	0.8698±0.0017	0.8675±0.0003
20	0.9986±0.0013	0.9971±0.0003	0.9681±0.0025	0.9651±0.0003	0.8984±0.0012	0.8972±0.0002
30	0.9925±0.0010	0.9954±0.0003	0.9665±0.0020	0.9690±0.0003	0.9386±0.0010	0.9378±0.0002
40	0.9935±0.0010	0.9945±0.0003	0.9772±0.0018	0.9786±0.0003	0.9754±0.0009	0.9757±0.0002
50	0.9952±0.0009	0.9964±0.0002	0.9918±0.0017	0.9922±0.0003	1.0028±0.0008	1.0033±0.0002
60	0.9992±0.0008	1.0005±0.0002	1.0069±0.0015	1.0058±0.0003	1.0217±0.0008	1.0218±0.0002
70	1.0048±0.0008	1.0057±0.0002	1.0173±0.0015	1.0179±0.0003	1.0333±0.0007	1.0344±0.0002
80	1.0117±0.0007	1.0121±0.0002	1.0266±0.0014	1.0268±0.0003	1.0413±0.0007	1.0432±0.0002
90	1.0155±0.0007	1.0155±0.0002	1.0298±0.0014	1.0310±0.0003	1.0462±0.0007	1.0470±0.0002
100	1.0102±0.0007	1.0110±0.0002	1.0256±0.0014	1.0265±0.0003	1.0414±0.0007	1.0433±0.0002
110	1.0034±0.0007	1.0045±0.0002	1.0157±0.0015	1.0178±0.0003	1.0323±0.0007	1.0340±0.0002
120	0.9964±0.0007	0.9983±0.0002	1.0039±0.0015	1.0056±0.0003	1.0186±0.0008	1.0208±0.0002
130	0.9911±0.0008	0.9922±0.0002	0.9887±0.0017	0.9913±0.0003	0.9990±0.0008	1.0011±0.0002
140	0.9865±0.0009	0.9881±0.0003	0.9738±0.0018	0.9761±0.0003	0.9704±0.0009	0.9723±0.0002
150	0.9856±0.0010	0.9876±0.0003	0.9637±0.0020	0.9650±0.0003	0.9330±0.0010	0.9320±0.0002
160	0.9866±0.0013	0.9886±0.0003	0.9583±0.0025	0.9593±0.0003	0.8885±0.0012	0.8874±0.0002
170	0.9906±0.0018	0.9923±0.0003	0.9585±0.0035	0.9601±0.0003	0.8558±0.0016	0.8519±0.0002
180	1.0009±0.0051	0.9973±0.0003	0.9594±0.0100	0.9661±0.0003	0.8488±0.0047	0.8498±0.0002

For the surface tally method the calculations were normalised by dividing the fluence in each segment by the total fluence through the 2 m radius sphere. Since the MCNP calculations are normalised to a single source neutron, the fluence for normalisation would be expected to be equal to the inverse of the total surface area of the sphere. In practice, the number was slightly greater, by about 1.4%. Breaking down the histories of the neutrons, and recording the losses and gains due to various capture, (n,xn), and fission reactions, revealed the reason for this increase. Although a small number of neutrons are lost to capture, the overall gains outweigh the losses and the net effect is a slight increase of the total number of neutrons emitted from the capsule over and above those produced by the (α,n) reactions. The majority of these extra neutrons come from fission events in the americium although there is also a very small component from (n,xn) reactions within the capsule.

In the next section the results of these calculations, and all other available calculations and measurements, are compared with the present measurements.

10. COMPARISON WITH CALCULATIONS AND PREVIOUS MEASUREMENTS

The results for the ^{252}Cf source in an X1 capsule, presented in Table 2 and Figure 7, have been published before[13], and are included here only for completeness, and for ease of comparison with other sources and encapsulations. The form of the ^{252}Cf isotope in X1 encapsulations can vary. In older sources, the ^{252}Cf was dispensed into the inner capsule in solution, and was evaporated to dryness, the californium being deposited as a mixture of oxides. This is not typical of modern ^{252}Cf sources, but was the case for the source whose measured data are shown in Figure 7. The anisotropy shown in this figure is therefore probably not typical of that for more recently produced sources.

Modern sources are usually constructed with the ^{252}Cf incorporated either in a palladium wire, or a ceramic bead, the bead tending to be used only for the lower activity sources. Because the bead or wire is smaller than the inner cavity it can move about within this volume. If a more fixed configuration is required, the source capsule can be manufactured with an inner bobbin to locate and fix the activity at the centre. An example of the anisotropy for such a source, where the ^{252}Cf, in the form of a wire, was fixed centrally, is shown in Figure 8 with the values listed in Table 3. The anisotropy is much more symmetrical about 90° than for the oxide source, and there is very much less variation in the anisotropy factors around the 90° direction.

A very detailed anisotropy measurement for an X1 encapsulated ^{252}Cf source has recently been reported by Kluge[14]. The results show a very smooth variation with angle, but no information is given about the form of the ^{252}Cf material within the capsule. The value quoted for $F_I(90°)$ is 1.016 ± 0.003 which indicates a similar, rather small, anisotropy factor at the waist to that given in Tables 2 and 3, i.e. 1.0103 ± 0.0011 and 1.0176 ± 0.0022 respectively.

Tables 4 and 5 and the corresponding Figures 9 and 10 give results for capsules designated X224 and SR-Cf-100 respectively. Both of these capsules had identical external dimensions, however, internally, and in terms of constructional materials, they were different.

For the X224 design the material of both the primary and outer encapsulations was stainless steel. The source material, in the form of a short length of palladium wire containing the ^{252}Cf isotope, was inserted into the inner cylindrical cavity of length about 18 mm and diameter roughly 4 mm, where it is free to move around, and can be at any position within the cavity. This fact may explain the rather asymmetric anisotropy factors shown in Figure 9, although, because the source had a rather low emission rate, the statistics on the measurements are poor. (X224 capsules where the ^{252}Cf material is more precisely positioned using internal spacers, can be obtained if requested from the manufacturer.)

The constructional materials of the SR-Cf-100 encapsulation were rather different, with an inner primary capsule of platinum (90%) and rhodium (10%) alloy, and an outer Zircalloy container[15]. The inner cavity contains porous platinum plugs which locate the ^{252}Cf material near the centre of the capsule.

A comparison of the anisotropy factors of the X224 and SR-Cf-100 sources is presented in Figure 24 where they are also compared with a calculation for the SR-Cf-100 type capsule performed using the Monte Carlo code MCNP by Hertel and McDonald[15]. There is rather good agreement between the SR-Cf-100 measurement and the calculation, particularly in the important angular range around 90°. In the region around 0° and 180°, however, the lack of angular resolution in the calculation makes the comparison difficult. The large length to diameter ratio for these source capsules makes the anisotropy quite pronounced, although the 90° anisotropy factor appears a little less for the X224 capsule than for the SR-Cf-100.

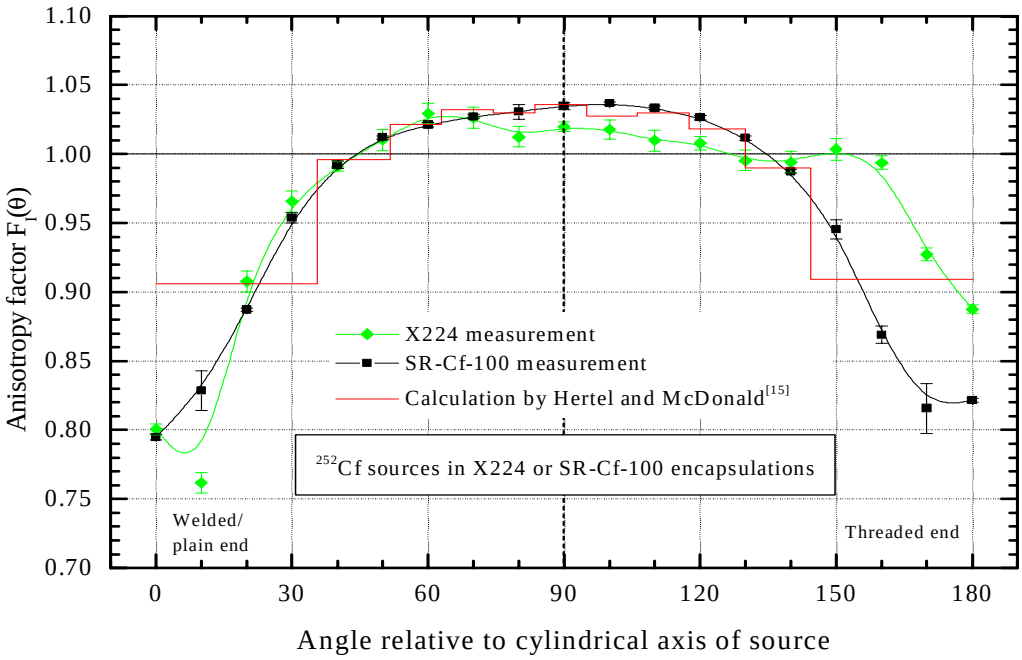

Figure 24. Comparison of measurements and calculation for the anisotropy of ^{252}Cf sources in X224 and Sr-Cf-100 capsules.

In a recent paper by Kim et al[16] some further calculations for this type of encapsulation are reported. Although the capsule is described as an SR-Cf-100, the calculations were performed with the Zircalloy outer capsule replaced with stainless steel. The only number presented for the anisotropy is $F_I(90°)$. For two calculational approaches described as: an angular bin tally (the same as the present surface tally), and a ring detector tally, the $F_I(90°)$ values were 1.0223 and 1.0337 respectively. These can be compared with 1.035 ± 0.31% and 1.034 ± 0.07% quoted by Hertel and McDonald for the corresponding calculational approaches, and the present measured values 1.0348 ± 0.0026 and 1.0198 ± 0.0034 for the SR-Cf-100 and the X224 measurements.

Figure 25 presents a comparison between the present measurement and the present MCNP calculation for an ^{241}Am-Be source in an X2 encapsulation. The agreement between measurement and calculation is unfortunately not very good. The measurement was performed with a 100 mCi source, the emission rate was thus low, and the statistical accuracy is not particularly high.

Nevertheless, the overall disagreement is outside what would be expected on statistical grounds. In particular the measured anisotropy factors at small angles are very much higher than the calculation, and are in fact higher than the measured factor at 90°. In view of the geometry of the source this seems rather unlikely, and the calculations appear more reliable. Although the overall agreement is poor, there is reasonable agreement for the important parameter, i.e. $F_I(90°)$, the measured value being 1.0112 ± 0.0037 and the calculated value being 1.0148 ± 0.0010.

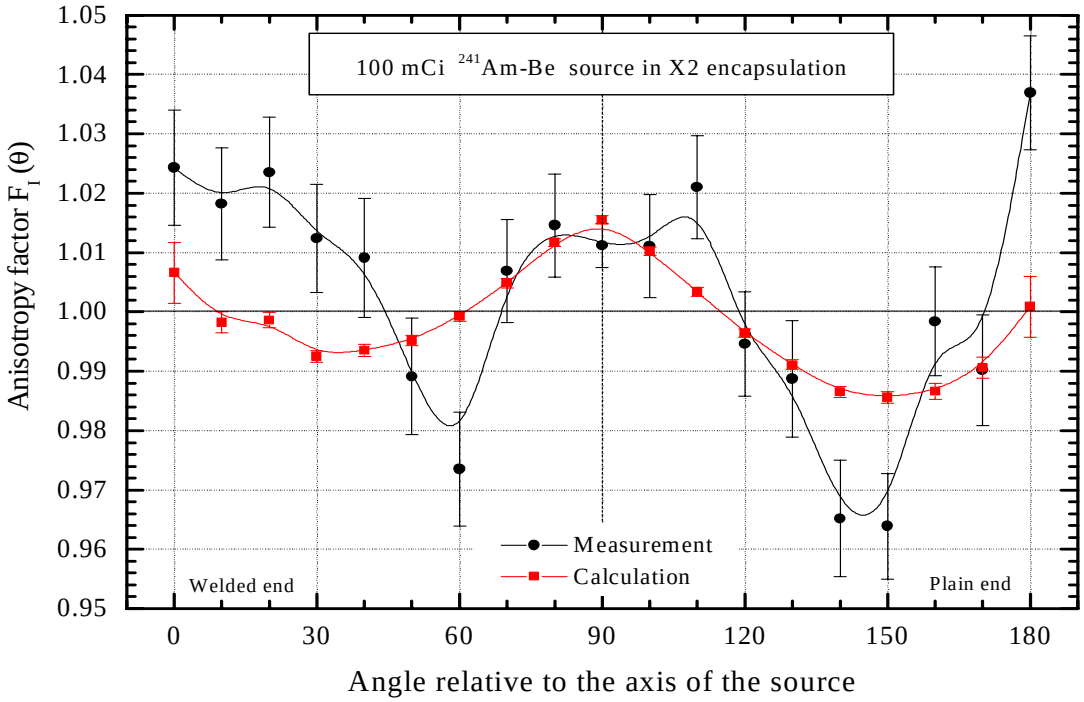

Figure 25. Comparison of measurement and calculation for the anisotropy of an ^{241}Am-Be source in an X2 capsule.

For ^{241}Am-Be sources in X3 type encapsulation measurements were performed for two different sources, both of which contained 1 Ci of americium. The results are shown in Figure 26 where it can be seen that the anisotropies of both sources are very similar. There may be some possible slight differences near the 180° end of the source, but in general the measurements are identical within the uncertainties. Also shown in this figure are the MCNP calculations which show remarkable agreement with the measurements. For the calculation, neutron production was assumed to be uniform within the volume containing the americium/beryllium mixture. The $F_I(90°)$ factors were: source capsule (A) 1.0276 ± 0.0028, source capsule (B) 1.0265 ± 0.0037, and calculation 1.0298 ± 0.0014. Calculated values for $F_I(90°)$ for this source are also given by Kim et al.[16], and these are 1.0272 and 1.0315 for the angular and ring tallies respectively. Although no uncertainties are given, these numbers are very similar to the present measurements and calculations.

In Figure 27 the results for two measurements and two MCNP calculations of the anisotropy of ^{241}Am-Be sources in X4 type encapsulation are shown. One of the measurements is from the present work, and the other measurement, and the calculations, are from the paper by Kim et al.[16]. One of the calculations uses an angular bin tally, while the other uses a ring detector tally. Data were extracted graphically from a figure in this paper, and no uncertainties are shown there. The measurements were performed using a long counter, and although it is not stated explicitly in the paper, 0E corresponds to emission through the welded (threaded recess) end[17].

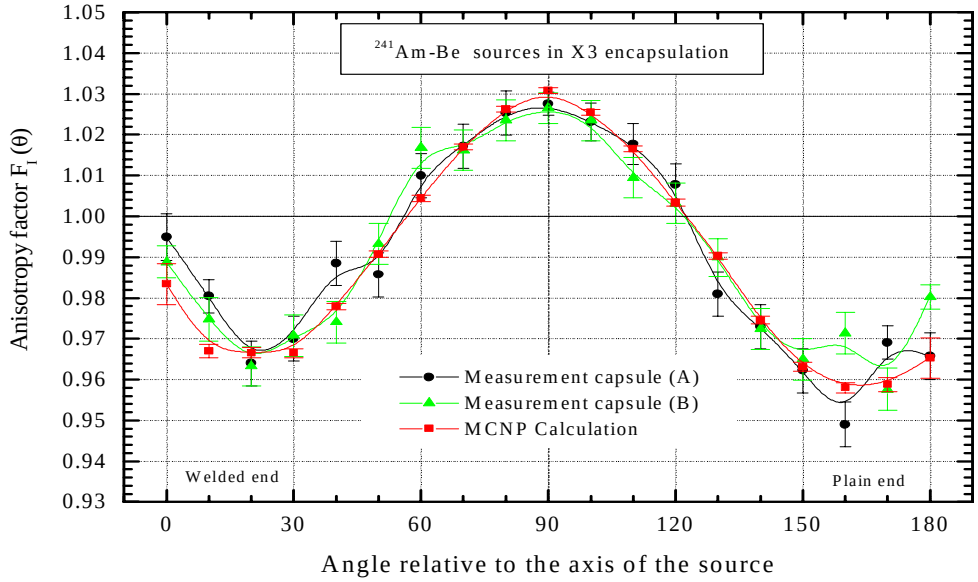

Figure 26. Comparison of measurements and calculation for the anisotropy of ^{241}Am-Be sources in X3 capsules.

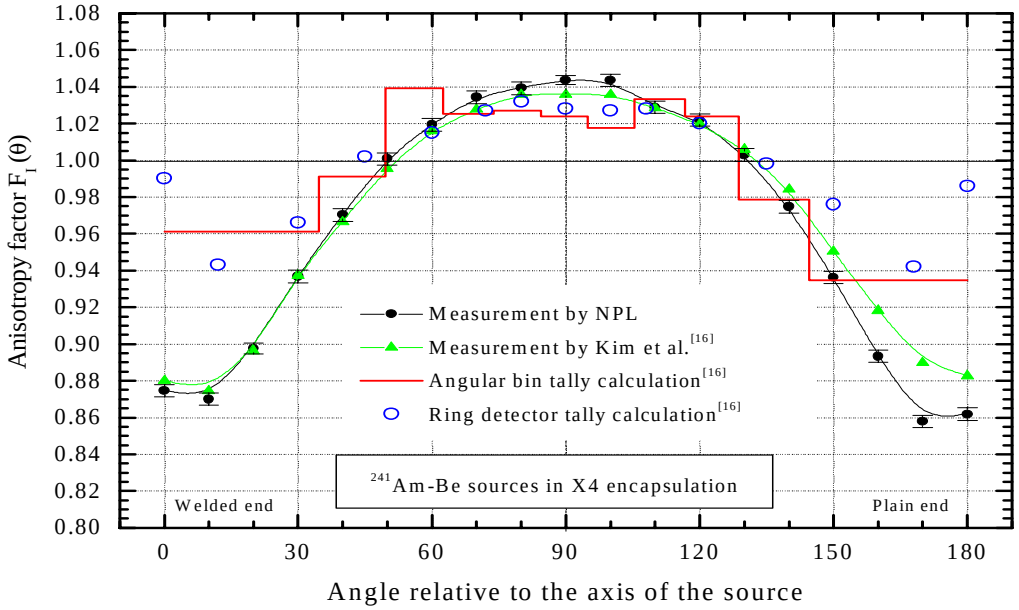

Figure 27. Comparison of measurements and calculation for the anisotropy of ^{241}Am-Be sources in X4 capsules.

The measurements agree reasonably well, although there is some suggestion that the source measured at NPL has marginally more anisotropic an output. The calculations, particularly that using the ring detector, appears to underestimate the degree of anisotropy compared to the measurements. Values for $F_1(90°)$ were: present measurement 1.0436 ± 0.0025, Kim et al.[16] 1.0363 for the measurement, and 1.0194 and 1.0285 for the angular and ring tally calculations respectively.

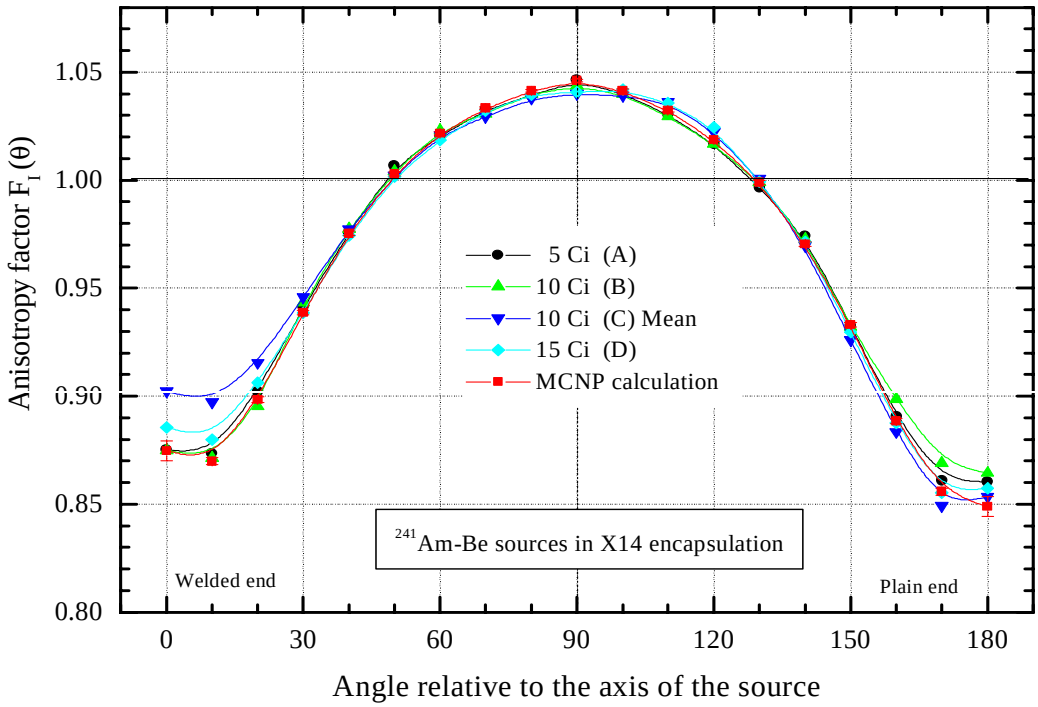

Figure 28. Comparison of measurements and calculations for the anisotropy of ^{241}Am-Be sources in X14 capsules.

Figure 28 presents experimental results for X14 capsules containing different amounts of americium. Two of the capsules contained 10 Ci of americium, one contained 5 Ci, and one contained 15 Ci. Uncertainties for these measurements are not included in this figure to avoid confusion between the data point for the different sources. All four sources have very similar anisotropies, although one of the 10 Ci sources, (C), is less symmetrical about 90° than the others, having a higher output through the 0° end. This effect is not an error in the measurement as the anisotropy for this source has been measured three times since 1989 with very consistent results as illustrated in Figure 29.

Rao et al.[18] have published anisotropy factors for five different sources. They do not identify any of these by giving encapsulation types, however, they do give the dimensions of the capsules, from which it would appear that one of these is an X14 capsule housing a 5 Ci ^{241}Am-Be source. (None of the other capsules match any of those reported here.) Values are presented for $F_I(90°)$ and $F_I(0°)$ although it is not clear which end of the capsule corresponds to 0°. The factors for the 5 Ci source are 1.05 ± 0.01 and 0.81 ± 0.01 at 90° and 0° respectively, and these are in broad agreement with the present measurements although the 0° result is somewhat lower.

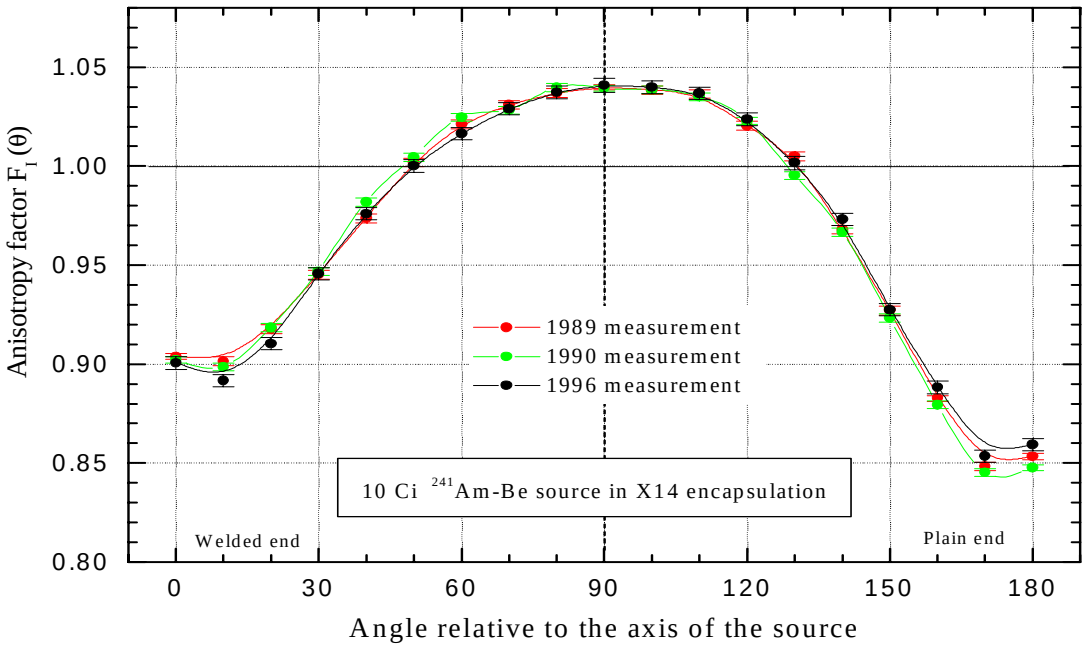

Figure 29. Comparison of three measurements of the anisotropy of X14 10 Ci ^{241}Am-Be source (C) performed between 1989 and 1996 showing excellent reproducibility.

Anisotropy values for a 5 Ci source in an X14 capsule have been determined by Jósefowicz et al.[19], and the factor derived at 90° was 1.035 ± 0.007. This is in agreement, within the uncertainties, with the present value, but the measurements were performed, not with a long counter but with a Studsvik 2202D area survey instrument. Because the neutron spectrum is not expected to change significantly with angle, the use of an area survey instrument should not give significantly different results.

The results of the present MCNP calculation are shown in Figure 28 where they can be compared with the various measurements. The agreement appears to be remarkably good. For the calculation the density of the ^{241}Am and beryllium mixture was derived from a knowledge of the volume of the central cavity of the source, and a typical figure for the weight of the mixture. The calculated anisotropy depends on this density, the degree of anisotropy increasing as the density is increased. The value used for the density appears to be about right. The X14 source is, however, constructed from three separate pellets of the ^{241}Am/Be mixture, and by altering the densities of individual pellets the anisotropy of source (C), which has a higher output through the 0° end than the other sources, can also be replicated. This effect could, however, also be the result of different ^{241}Am to Be ratios in the different pellets.

No comparison with calculation was possible for the other sources, ^{241}Am-B, ^{241}Am-F, ^{241}Am-Li, and ^{239}Pu-Li, whose measured anisotropies are presented here. Calculations for these are a little more problematical because the spectra are not so well characterised. A comparison of the plots of their measured anisotropy factors, however, reveals certain generally expected features. Anisotropy is expected to increase as: the source mean energy decreases, the amount of source material within the capsule increases, and also as the length to diameter ratio of the cylindrical source capsule increases. It is not surprising therefore that the ^{241}Am-Li source, which has the

lowest mean energy, when contained in an X14 capsule, exhibits the highest degree of anisotropy for any of the sources. Emission through the 0° end of this capsule is only about 64% of the emission at the waist, i.e. at 90°.

11. MEASUREMENTS AROUND THE CYLINDRICAL AXIS OF THE SOURCE

In the preceding work it has been assumed throughout that the neutron emission from each source was symmetrical about the cylindrical axis of the source. In order to check the validity of this assumption measurements of the variation of neutron emission in directions perpendicular to the axis were made on the physically largest source capsule available, the particular source chosen being a 10 Ci ^{241}Am-Be source enclosed in an X14 capsule. Any variation of neutron emission in a radial direction, due to uneven distribution of the source material, ^{241}Am activity or target Be, or because of voids in the compacted powder, is likely to be more evident in such a large source. The source has a nominal emission rate of 2.5 H 10^7 s^{-1}.

The source was placed in a thin-walled cup mounted on an extended 6 mm diameter stem with the cylindrical axis held vertically by means of a small 3-jaw chuck attached to the end of a flexible drive shaft. The inner shaft of the flexible drive was rotated in 24° steps by means of a hand crank via a 30:1 reduction gearbox. Two revolutions of the hand crank resulted in a 24° rotation of the source about its cylindrical axis. The source was positioned at the centre of the NPL low-scatter area with its active centre at the same height as the axis of the NPL standard long-counter which was positioned with its front face 2.058 m from the axis of the source.

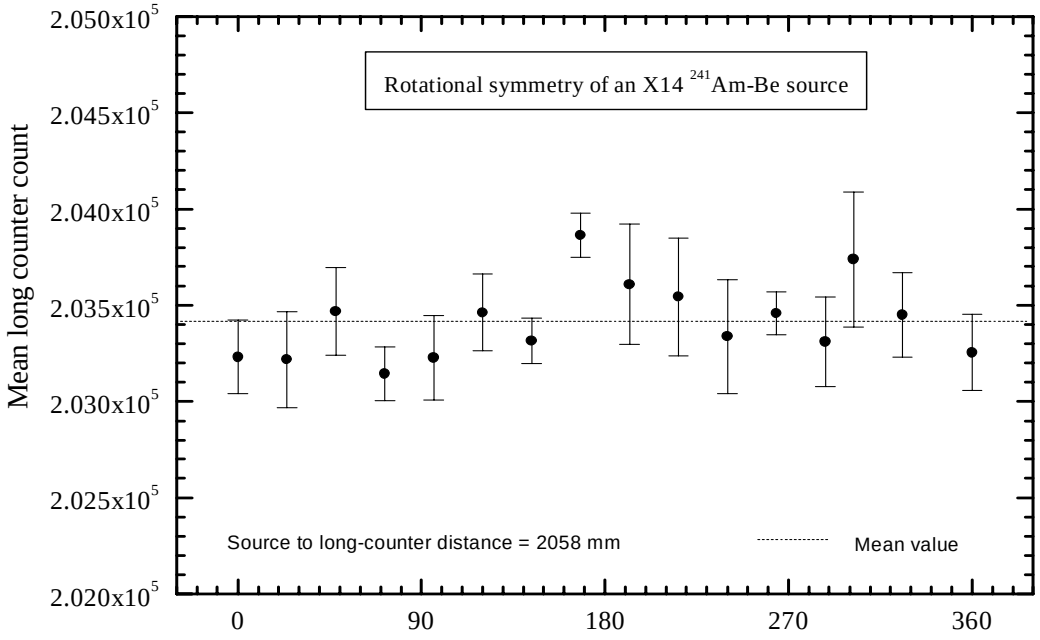

Figure 30. Rotational symmetry of emission for an X14 ^{241}Am-Be source.

A number of measurements for 400 s counting periods were accumulated at each 24° step from 0° to 360° of rotation. The source was viewed through a surveyor's level at each angle of rotation and was observed to move laterally by an estimated 1 mm in the course of one 360° rotation. This was assumed to be due to the difficulty in ensuring that the flexible drive unit and the stem were co-linear and truly vertical, resulting in the centre of the source precessing on an estimated 1 mm diameter path about the point of rotation. These variations will affect the long counter readings by only 0.1%, however, corrections were applied for this effect.

No corrections were made for counting dead-time, background or room-scattered neutrons on the assumption that these corrections would be constant for all angles of rotation if the neutron emission was isotropic in the equatorial plane and the long-counter was held in a fixed position in the measurement room.

The mean count rate for each angle was calculated and was corrected only for the apparent lateral movement of the source. The corrected counts together with their associated standard errors are shown in Figure 30. It can be seen that the neutron emission about the cylindrical axis of the source is symmetrical, within the indicated uncertainties, for all angles, and that the assumption of symmetry about this axis is valid for this source. It is also most probably valid for all similarly constructed ^{241}Am-Be sources. For ^{252}Cf sources this may not always be the case, because of the small amount of ^{252}Cf material involved, which may be at any position within the central cavity.

12. DISCUSSION AND CONCLUSIONS

Radionuclide sources are extensively used for calibrating neutron sensitive devices. In these calibrations the number of neutrons arriving at the device is derived by assuming a inverse square law dependence of the fluence on the source to device distance making it, in principle, very simple to calculate the fluence at any distance, provided the total emission rate of the source and the anisotropy of emission are known. The total emission rate from such sources can be measured with an uncertainty as low as 0.6% at the 1σ level. Room scatter effects need to be taken into consideration, but for rooms where the scatter is small, or has been very well characterised, the correction can be well known. In such situations, a lack of any knowledge of the anisotropy of the source emission as a function of angle can represent by far the largest contribution to the uncertainty in the fluence at a device. Even where the anisotropy factors are known, the uncertainty in the value can still be a major contribution to the uncertainty in the fluence.

In some situations the very highest accuracy is required. For example, radionuclide sources are used to calibrate instruments subsequently used to measure and standardise monoenergetic neutron fluences[20]. For these applications it is important that the source anisotropy is known accurately and measurements on the particular sources used is always to be recommended.

Although calibrations of area survey instruments rarely need to be performed to the highest accuracy, 5 to 10% usually being considered adequate, laboratories can do better. In particular, they expect to do better in intercomparisons of calibrations at different laboratories where they expect agreement within the quoted uncertainties. Surprisingly, very few determinations of source anisotropy have been reported in the open literature, so anisotropy corrections are often poorly known and in some situations are not even applied. Considerable time can be wasted in identifying the reason for disagreements in such cases.

For personal dosemeters there is a requirement in many countries that their response is correct to within particular limits. The response is checked using radionuclide sources, and ignoring anisotropy effects, or using inappropriate values, could possibly push the dosemeter performance over the dividing line between being acceptable and not being acceptable. This would have serious consequences for the service providing these personal dosemeters.

This report contains probably the most extensive set of radionuclide neutron source anisotropy measurement data presently available. These are summarised in Table 19 where the 0°, 90°, and 180° anisotropy factors are listed for all the sources measured. For the X3 and X14 encapsulations more than one source has been measured, and a comparison of the results provides some information on how reproducible the anisotropy factors are between sources of the same type and the same encapsulation. For the two X3 capsules the anisotropies were very similar. In the case of the X14 encapsulated sources there was more variation. No information is available for other source encapsulations. Nevertheless, the values given in this report provide what are, in most cases, the best available estimates of the anisotropies, and these should be applicable for sources of the same type in the same encapsulation in the majority of applications. If, however, these values are used in this way some increase in the uncertainty should be made to allow for the differences which can occur even between sources of the same encapsulation and type.

Table 19. Summary of measured anisotropy factors at 0°, 90°, and 180° for all sources in this report.

Source type	Nominal activity or mass	Encapsulation style	Diameter (mm)	Height (mm)	Nominal neutron emission rate (s^{-1})	$F_I(0°)$	$F_I(90°)$	$F_I(180°)$
^{252}Cf (sp.fis.)	10 μg	X1 (A)	7.8	10.0	2.5 H 10^7	1.0267	1.0103	0.9745
^{252}Cf (sp.fis.)	10 μg	X1 (B)	7.8	10.0	2.5 H 10^7	1.0055	1.0176	1.0018
^{252}Cf (sp.fis.)	10 μg	X224 (A)	9.4	32.5	2.0 H 10^5	0.8877	1.0198	0.8005
^{252}Cf (sp.fis.)	17 μg	X224 (B)	9.4	32.5	4.0 H 10^7	0.7948	1.0348	0.8215
^{241}Am-Be (α,n)	100 mCi	X2	17.4	19.4	2.5 H 10^5	1.0243	1.0112	1.0369
^{241}Am-Be (α,n)	1 Ci	X3 (A)	22.4	31.0	2.5 H 10^6	0.9949	1.0276	0.9657
^{241}Am-Be (α,n)	1 Ci	X3 (B)	22.4	31.0	2.5 H 10^6	0.9888	1.0265	0.9802
^{241}Am-Be (α,n)	3 Ci	X4	22.4	48.5	7.5 H 10^7	0.8746	1.0436	0.8619
^{241}Am-Be (α,n)	5 Ci	X14 (A)	30.0	60.0	1.3 H 10^7	0.8752	1.0464	0.8603
^{241}Am-Be (α,n)	10 Ci	X14 (B)	30.0	60.0	2.5 H 10^7	0.8749	1.0436	0.8643
^{241}Am-Be (α,n)	10 Ci	X14 (C)	30.0	60.0	2.5 H 10^7	0.9005	1.0408	0.8593
^{241}Am-Be (α,n)	15 Ci	X14 (D)	30.0	60.0	3.8 H 10^7	0.8855	1.0407	0.8573
^{241}Am-B (α,n)	1 Ci	X3	22.4	31.0	4.4 H 10^5	0.9839	1.0345	0.9583
^{241}Am-F (α,n)	1 Ci	X3	22.4	31.0	1.4 H 10^5	0.9838	1.0224	0.9532
^{241}Am-Li (α,n)	5 Ci	X14	30.0	60.0	2.1 H 10^5	0.6899	1.0760	0.7633
^{239}Pu-Li (α,n)	17 Ci	2729-C	38.0	52.3	1.1 H 10^6	0.8532	1.0777	0.8138

For the majority of sources in X3, X4, and X14 capsules both the measurements and the calculations indicate a somewhat higher emission through the welded end, i.e. the screw threaded end, than the plain end. The slightly greater thickness of steel for the outer capsule at the plain end is a possible explanation for this. For the ^{241}Am-Li source in an X14 capsule the trend is, however, reversed with output higher through the plain end than the screw threaded end. There appears to be no obvious reason why this should be the case.

For the X3 and X14 encapsulations the agreement between the measurements and the present calculations is remarkably good; as is the agreement between the two calculational methods. It appears that MCNP can calculate the anisotropy of such sources rather well. Before such calculations can be performed, however, the constructional details of the source need to be known and modelled precisely. Relatively small errors in the model can result in the calculation being quite inaccurate. In fact, the calculated results are so sensitive to constructional details that a comparison between calculation and measurement can provide information on the internal constructional details of the source, e.g. the exact position and distribution of the neutron producing material. A good example of this is the comparison of calculation and measurement reported in reference 13 which provided information on the exact position of the ^{252}Cf within the inner capsule. For X14 capsule (C), where the agreement between measurement and calculation is not exact, see Figure 28, the computational model can be adjusted, by altering, for example, the densities of the three pellets of ^{241}Am/Be mixture from which the source is constructed, to give good agreement. This agreement can, however, be achieved with somewhat different combinations of densities for the three pellets. Furthermore, the effect may, in practice, be due to other effects, e.g. different ratios of ^{241}Am and Be in the mixtures, so it is difficult to derive unique information about the internal properties in this case.

The disagreement between measurement and calculation for the X2 source raises questions about the results. Bearing in mind that the capsule is even simpler to model than the X3 and X14 capsules, and the fact that there was good agreement obtained between measurement and calculation for the X3 and the X14 capsules, more confidence can probably be placed in the calculation than the measurement for this source. It certainly highlights the usefulness of simulations in verifying and gaining insight into the measurements.

Acknowledgements
We would like to thank AEA Technology QSA for providing detailed drawings of the X2, X3, and X14 capsules, Nicola Horwood for assistance with the data processing, and Graeme Taylor for help with some of the experimental work. We are grateful to Marconi Marine (VSEL) Limited for permission to use data for sources belonging to them. This work was funded by the UK National Measurement System Policy Unit and was Deliverable (iv) of Project 1.2 in its 1995 to 1998 Programme for Ionising Radiation Monitoring Metrology.

REFERENCES

[1] E.J.Axton and P.Cross, The Establishment of an Absolutely Calibrated Neutron Source, *Reactor Science and Technology. (Journal of Nuclear Energy, Parts A/B)* **15**, 22 - 27, 1961.

[2] E.J.Axton, P.Cross, J.C.Robertson, Calibration of the NPL Standard Ra-Be Photoneutron Sources by an Improved Manganese Sulphate Bath Technique, *Journal of Nuclear Energy Parts A/B* **19**, 409 - 422, 1965.

[3] E.J.Axton, Intercomparison of Neutron-Source Emission Rates (1979-1984), *Metrologia* **23,** 129-144, 1987.

[4] E.A.Lorch, Neutron Spectra of ^{241}Am/B, ^{241}Am/ Be, ^{241}Am/ F, ^{242}Cm/Be, ^{238}Pu/^{13}C and ^{252}Cf Isotopic Neutron Sources, *Int. J. App. Radiation and Isotopes*, **24**, 585-591, 1973.

[5] H.Kluge and K.Weise, The Neutron Energy Spectrum of a ^{241}Am-Be(α,n) Source and Resulting Mean Fluence to dose Equivalent Conversion Factors, *Radiation Protection Dosimetry,* **2**, 85-93, 1982.

[6] K.W.Geiger and L.Van der Zwan, Radioactive Neutron Source Spectra from ^{9}Be(α,n) Cross Section Data, *Health Physics*, **21**, 120-123, 1971.

[7] J.G.Owen, D.R.Weaver and J.Walker, Neutron Spectra from Am/F and Am/Li (α,n) Sources, *Proceedings Int. Conference on Nuclear Data for Science and Technology*, Antwerp.1982.

[8] W.Mannhart, Status of the Cf-252 Fission Neutron Spectrum Evaluation with Regards to Recent Experiments, *Proceedings IAEA Consultants= Meeting on the Physics of Neutron Emission in Fission*, Mito, Japan, 24-27 May, 1988, INDC(NDS) -220/L 305-336, Vienna, June 1989.

[9] International Standard ISO 8529, Neutron reference Radiations for Calibrating Neutron-Measuring Devices used for Radiation Protection Purposes and for Determining their Response as a Function of Neutron Energy, *International Organization for Standardization*, Geneva, Switzerland, 1989.

[10] J.B.Hunt, The Calibration and use of Long Counters for the Accurate Measurement of Neutron Flux density, *NPL Report RS 5,* April 1976.

[11] International Standard ISO 10647, Procedures for Calibrating and Determining the Response of Neutron-Measuring Devices used for Radiation Protection Purposes, *International Organization for Standardization,* Geneva, Switzerland, 1996.

[12] MCNP - A General Monte Carlo N-particle Transport Code, Version 4B, edited by Judith F Briesmeister, *RSIC, Oak Ridge National Laboratory. LANL Manual LA-12625-M Version 4B*, Los Alamos 1997.

[13] C.M.Eisenhauer and J.B.Hunt, Anisotropic Neutron Emission from a ^{252}Cf Source, *Radiation Protection Dosimetry,* **22**, 253-258, 1988.

[14] H.Kluge, Irradiation facility with radioactive reference neutron sources: Basic principles, *PTB-Report PTB-N-34*, Braunschweig, Juni, 1998.

[15] N.E.Hertel and J.C.McDonald, Calculations of Anisotropy Factors and Dose Equivalents for Unmoderated ^{252}Cf Sources, *Radiation Protection Dosimetry*, **32**, 77-82, 1990.

[16] B.H.Kim, J.L.Kim, S.Y.Chang, M.Do, and J.C.McDonald, Calculation and Measurement of Anisotropy Factors for Some Radioactive Neutron Sources, *Proceedings of the International Conference on Radiation Dosimetry and Safety*, Taipai, Taiwan, ROC, 31 March - 2 April, 1997.

[17] B.H.Kim, private communication, November 1998.

[18] U.S.Rao, A.Kumar, S.C.Misra, P.S.Nagarajan, U.C.Gupta. Anisotropic Neutron Emission from Laboratory Sources, *Nuclear Instruments and Methods*, **155**, 249 - 252, 1978.

[19] K.Jósefowicz, N.Golnik and M.Zielczy│ski, Dosimetric Parameters of Simple Neutron + Gamma Fields for Calibration of Radiation Protection instruments, *Radiation Protection Dosimetry*, **44**, No. 1/4, 139-142, 1992.

[20] H.Tagziria and D.J.Thomas, Re-calibration and Monte Carlo Modelling of the NPL Long Counters, *NPL Report CIRM 19*, October 1998.

****